Journal of Advanced Joining Processes 10 (2024) 100262

Contents lists available at ScienceDirect

Journal of Advanced Joining Processes

journal homepage: www.sciencedirect.com/journal/journal-of-advanced-joining-processes

Investigation of the electrical quality and long-term stability of aluminum ground stud connections in automotive applications

Viktor Haak, Keke Yang *, Gerson Meschut

Laboratory for Material and Joining Technology (LWF), Paderborn University, Pohlweg 47-49, 33098 Paderborn, Germany

ARTICLE INFO

Keywords:
Stud welding
Aluminum
Grounding connection
Electrical resistance
Superimposed load

ABSTRACT

The rapid advancement in the electrification of modern vehicles has led to a continuous increase in electrical consumers for various comfort and safety functions. Ground studs serve as the electrical interface between the conductive vehicle body and the onboard network. Drawn arc stud welding is an economical and established joining process for producing ground stud joints. The circuits in the onboard network are increasingly subject to greater demands regarding current-carrying capacity and long-term stability. Reliable signal and power transmission require minimal contact resistance at the electrical connection points of the ground stud system and must withstand various operating and environmental conditions over the entire service life. In this study, a ground stud made of AlMg5, with a ZnNi-coated steel cap nut was used on a 2.0 mm thick sheet of AlMg3. The electrical connection of the ground studs was made using tinned copper cable lugs and 35 mm^2 cables. To analyze the electrical resistance behavior in an accelerated test, the ground studs were subjected to a superimposed load with a cyclic current profile for 1008 h under changing climatic conditions. The results show that under the chosen operational and environmental conditions, accelerated aging and intermittent resistance behavior occur. A characteristic drop in resistance during the test indicates the failure point of the electrical connection. The cause of failure can be attributed to media penetration into the electrical contact zone. A failure of the electrical connection was observed after 512 h.

Introduction

To address energy and environmental issues, developing high-performance and cost-effective structures has long been a goal in engineering (Geng et al., 2021a,b; Hu et al., 2021). This goal is particularly evident in the automotive industry, where the increased use of lightweight materials reduces vehicle weight, thereby lowering emissions and meeting increasingly stringent CO_2 reduction regulations (Robinson et al., 2019; Emadi et al., 2022). In particular, the demand for lightweight solutions has highlighted the importance of using materials with high strength-to-weight ratios, especially in the automotive industry (Wu et al., 2018; Xia et al., 2020). Aluminum alloy materials, with their high specific strength, excellent processing performance, and recyclability, offer significant lightweight potential (Xian et al., 2019; Yang et al., 2022). Replacing some traditional steel components with aluminum alloys can achieve weight reduction without sacrificing the strength or structural stiffness of the vehicle body (Zhang et al., 2022; Li et al., 2019; Sun et al., 2021; Hirsch, 2014). This aligns with the design philosophy of using the right material in the right form for the right place (Taub and Luo, 2015). Examples of aluminum-intensive vehicle bodies include the Audi A8 D5 and Cadillac CT6, which use 58 % and 62 % aluminum alloys in their body structures, respectively. Additionally, this is crucial for increasing range in the context of e-mobility and ensuring the crash safety of battery housings (Czerwinski, 2021; Sanguesa et al., 2021; Scrosati et al., 2015).

The electrification of modern vehicles increases the number of electrical consumers that enable various comfort and safety functions (Kohler et al., 2011), such as air conditioning, electric seat adjustment, and assistance and information applications. With the current range of functions, the conventional 12-volt onboard network has already reached its performance limits. Consequently, increasingly higher currents are required at a constant 12-volt network voltage. The resulting current heating necessitates increasingly larger cable cross-sections (Spahr, 2017). The solution to ensuring increased power requirements,

Abbreviations: AC, Alternating Current; DC, Direct Current; DASW, Drawn Arc Stud Welding; EDX, Energy Dispersive X-ray Spectroscopy; SEM, Scanning Electron Microscopy.

* Corresponding author.
E-mail address: keke.yang@lwf.upb.de (K. Yang).

https://doi.org/10.1016/j.jajp.2024.100262

Available online 16 October 2024

especially with regard to e-mobility and autonomous driving, is the integration of a second partial onboard network with 48-volt technology, which supplements the 12-volt onboard network. This opens up numerous new applications with powerful functions, such as brake energy recovery (recuperation), driver assistance systems (e.g., automatic steering), and electrically driven compressors. Consequently, both the complexity of the onboard network and the number of necessary electrical ground connection points in the vehicle increase. An important component of every vehicle body is ground studs, which serve as an electrical interface between the vehicle body and the onboard network. The connection of electrical consumers is made by mounting tinned copper cable lugs to the ground studs attached to the vehicle body. In automotive engineering, functional elements, e.g. self-piercing studs (Füssel et al., 2022) or weld studs (Ramasamy, 2000; Reis and Braun, 2024) are used in many cases. Due to the numerous advantages of welded joints compared to mechanical joints, drawn arc stud welding (DASW) is often used for aluminum applications related to electrical contacting in automotive engineering (Reis and Braun, 2024). DASW is used to produce an inseparable, material-locking ground connection on aluminum components. This ensures mechanically and electrically robust current transmission (Reis and Braun, 2024). The welding process is characterized by a very short process time, one-sided accessibility to the joint, and a high degree of automation (Vural, 2014; Hsu, 2015). DASW is therefore a very economical and established welding process for joining solutions in the automotive industry (Ramasamy, 2002). A schematic of the AC-process for aluminum applications is shown in Fig. 1.

Aluminum alloys are particularly suitable for current transport due to their good electrical and thermal conductivity (Ostermann, 1998; Lumley, 2011). Electrical conductivity depends on both the alloy composition and the heat treatment condition (Ostermann, 1998). Due to their high oxygen affinity, a natural oxide layer (Al_2O_3) quickly forms on the aluminum surface even under normal environmental conditions (Ostermann, 2014). The oxide layer is a very thin, dense, firmly adhering, amorphous protective layer with very low electron and ion conductivity (Ostermann, 2014). The composition, thickness, and electrical resistance of the oxide layer depend on the alloy composition, manufacturing process, and storage and processing conditions (Ostermann, 2014). The growth rate and thickness of the oxide layer increase with humidity (Godard, 1967) and elevated temperature (Hunter and Fowle, 1956). In electrical connections, these characteristics of aluminum alloys pose additional challenges. The circuits in the onboard network are increasingly subject to high demands regarding current-carrying capacity and long-term stability. Reliable signal and power transmission play a central role, especially in the context of e-mobility and autonomous driving.

For current transmission, minimal contact resistance at the electrical connection points is desired over the entire lifespan. This resistance is influenced by several factors such as connection geometry, contact force, temperature, and material. It increases over the operational period due to various aging mechanisms, including force degradation, foreign layer formation, electromigration, fretting corrosion and interdiffusion (Schlegel et al., 2012; Braunovic, 2009; Oberg et al., 1996; Hildmann, 2017). These different aging mechanisms generally occur simultaneously. Depending on the type of connection, the materials used, the electrical load, and the environmental conditions, different mechanisms may dominate the aging process. All mechanisms are highly temperature-dependent - the higher the temperature the faster the electrical connections ageing (Hildmann, 2017; Pfeifer, 2015). Fig. 2 shows a schematic of the aging-related progression of contact resistance, divided into various phase sections of the lifecycle curve (Schlegel et al., 2022). The so-called intermittent phase describes a phased, unstable resistance behavior that marks the failure of the electrical connection since reliable electrical function can no longer be ensured. It is known

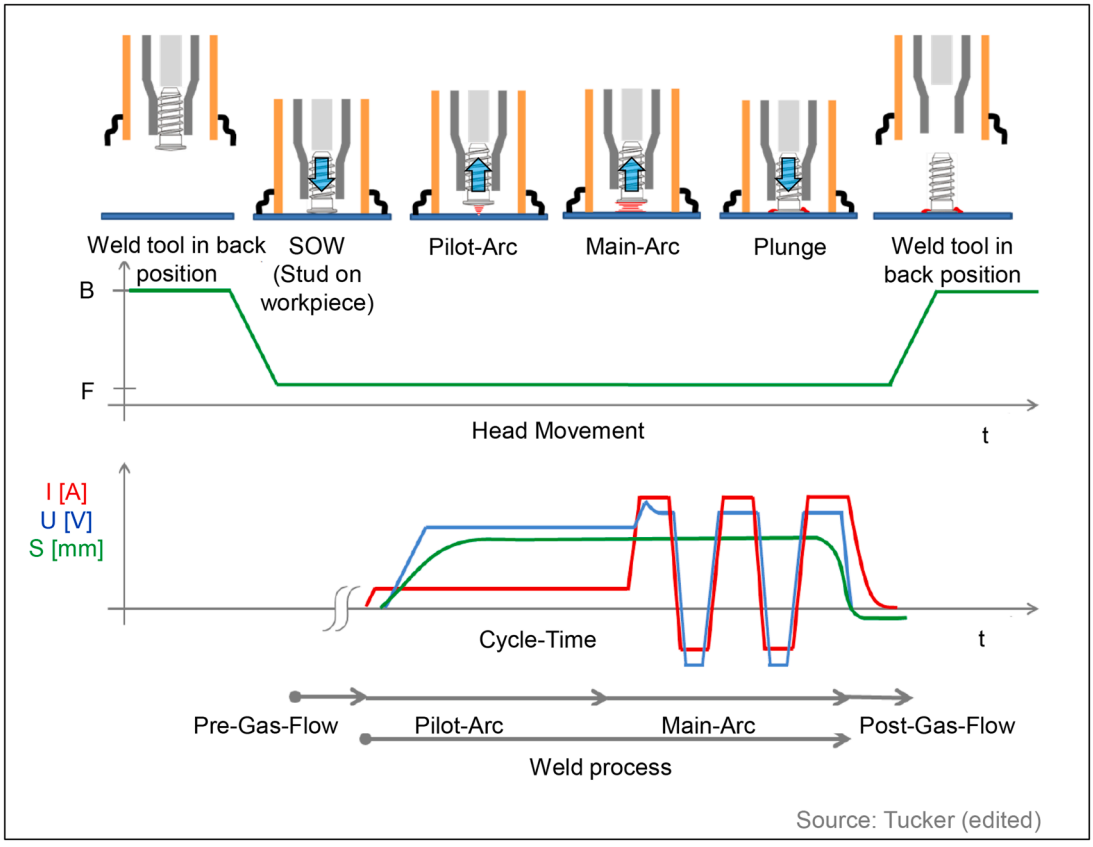

Fig. 1. Schematic drawn arc stud welding AC-process for aluminum application according to (Reis and Braun, 2024).

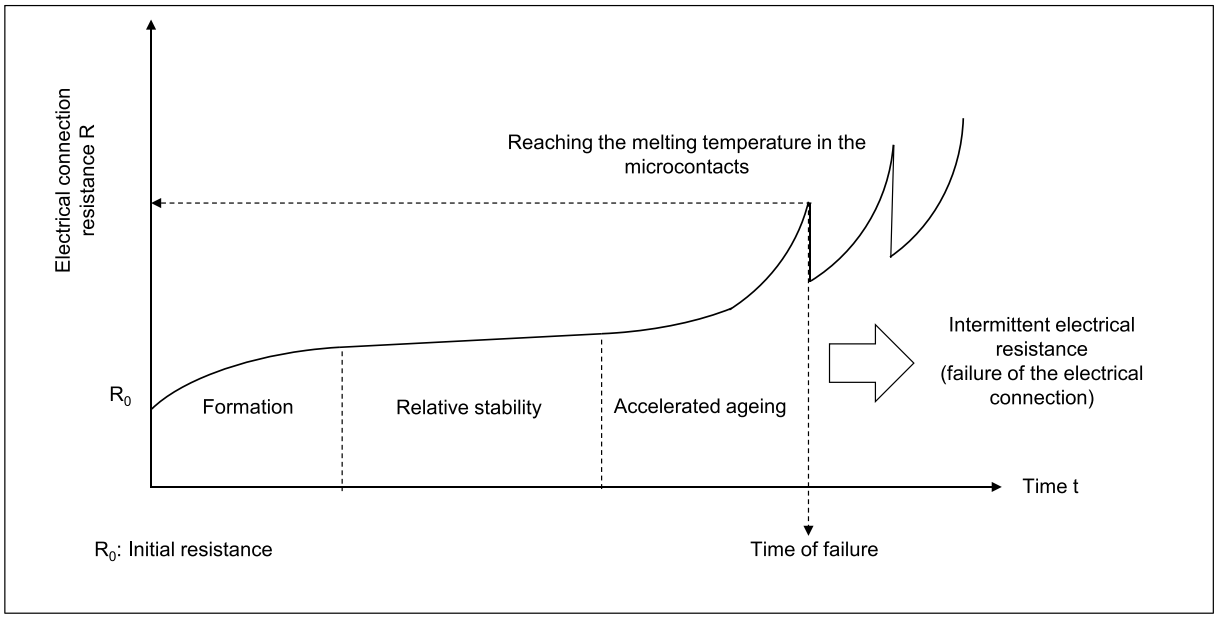

Fig. 2. Service life characteristic of an electrical connection according to (Schlegel et al., 2022; Bergmann, 1996).

from power engineering that the onset of intermittence is related to the melting temperature reached at the microcontacts (Schlegel et al., 2022; Bergmann, 1996).

The growing market for electric and hybrid vehicles is leading to an increasing number of vehicles with complex onboard network systems. As vehicle electrification increases, the need for reliable electrical contacts and systems is becoming ever more important. A common measure for the reliability of onboard network components is the failure rate (FIT: Failure In Time). The failure rate is the time-averaged frequency of an observed failure. Currently, no statements can be made regarding failure models and failure rates for ground stud connections, as there is insufficient data from field observations (ZVEI e.V. und Bayern Innovativ GmbH 2024). Among the most commonly used types of contacts in the automotive industry are electrical connectors, which represent typical separable electrical contacts in the onboard network. Song et al. (2018) examined the reliability of electrical connectors using accelerated lifetime tests characterized by thermal and mechanical loads. The reliability, based on the failure rate, is investigated under varying vibration and thermal cycle loads and represented by a model predicting the failure rate. Kloch et al. (2021) studied electrical connectors with a focus on the fretting phenomenon, which is caused by microscopic movements between contact surfaces. The investigations to predict performance and durability include dynamic tests (shock test, vibration test), humidity and temperature tests (temperature shock, splash water) and numerical modeling approaches. In addition to examining individual components, comprehensive studies have also analyzed real-world applications and their failure mechanisms. In an extensive study by Hilmert et al. (2022), electrical connectors in field vehicles from various automotive manufacturers were analyzed for different failure mechanisms, and their frequency was statistically evaluated. It was found that the most common main causes of electrical connector failures in long-term use are fretting corrosion and oxidation of the contact surface, as well as wear of the often-tinned surfaces. Rachman et al. (2013) investigated the influence of contact pressure and surface roughness of uncoated, nickel-plated, and silver-plated copper connectors and found that the resulting contact resistance is influenced not only by the specific resistance of the contact material but also by the surface topography and roughness. Braunovic (1981) investigated the impact of cyclic current loads on bolted aluminum connections and observed a drastic loss of contact force. Schneider et al. (2009) showed in their study of Al-Cu busbar connections at an aging temperature of 140 °C that uncoated contact surfaces of Al-Cu connections have a significantly shorter lifespan compared to pure connections (e.g., Al-Al or Cu-Cu connections). This is due to the formation of intermetallic phases, the ingress of foreign layers into the microcontacts, and displacement movements (fretting). Galvanic corrosion is considered one of the most dangerous degradation mechanisms in a bimetallic system. Sampaio et al. (2022) investigated the influence of corrosion (salt spray test) on the electrical and mechanical performance of hybrid busbars made of aluminum and copper. The study demonstrated that electrical connection resistance increases over time due to corrosion, particularly in busbars with conventional bolted connections (M8 bolt-nut pair made of carbon steel). It was found that in bolted connections, especially those with a low tightening torque, the penetration of the salt solution and the formation of corrosion products at the connection points led to a significant increase in resistance. In a study by Pan et al. (2021), resistance spot welded joints and self-pierce riveted joints of an aluminum-steel combination were examined for corrosion behavior using a salt spray test. The results showed that the gap created in the overlap area as a result of the joining process had a significant influence on the corrosion behavior. The larger gap in the resistance spot welded joint led to an increased corrosion rate in the overlapped area, while less corrosion occurred in the self-pierce riveted joint due to the significantly smaller gap.

In this context, both the basic evaluation of electrical quality and the understanding of the aging-related long-term behavior of ground stud systems are of great importance. According to the current state of technology and research, there are no standards or unified guidelines for the electrical quality assessment and evaluation of the long-term behavior of ground stud connections. The condition of an electrical connection can generally be determined by its electrical resistance. Therefore, in this study, the resistance-time profile of the examined ground stud system is analyzed under intensive stress in the form of an electrically-medially/corrosively induced load. The test setup used enables a basic evaluation of the electrical connection quality of ground stud systems and provides insight into their long-term stability under the environmental and operating conditions considered in this study.

Materials and methods

Materials and ground studs

In this study, an aluminum wrought alloy of type AlMg3, conforming

to [DIN EN 573–3], in the O/H111 temper and with a thickness of 2.0 mm, was used according to [DIN EN 485–2]. The chemical composition and mechanical properties are shown in Tables 1 and 2.

A cold-headed ground stud made from an aluminum alloy (AlMg5), conforming to [DIN EN 573–3] in temper H32 was used, according to [DIN EN 1301–2]. This ground stud with a metric thread of dimension M8 is typically applied in the automotive industry and is welded to aluminum structures (e.g., sheet metal, extruded profile, die casting) using drawn arc stud welding. The ground stud is delivered and welded in a completed form. The ZnNi-coated steel cap nut (strength class 8) is already screwed onto the aluminum ground stud (Fig. 3). The surface of the aluminum ground stud is provided with a titanium conversion coating.

The chemical composition and mechanical properties of the alloy, which are crucial for determining the performance and reliability of the ground stud in automotive applications, are shown in Tables 3 and 4.

SEM/EDX analyses were conducted to examine the electrical contact surfaces in more detail. This method enables the identification of chemical elements on the contact surface. Fig. 4 presents the results of the EDX analysis for the contact surface of the ground stud components. The overview image (top row) highlights the area of analysis (yellow frame). It is evident that the aluminum surface has “spots” in some areas, which were identified as zinc and nickel residues. These residues originate from the ZnNi coating of the steel cap nut and are due to the fitting of the nut to the stud. The influence of this fitting process is also visible on the surface of the steel cap nut. In this case, the nut substrate material (iron) was detected in the inner edge area, indicating damage to the ZnNi coating, which consequently led to increased deposition of aluminum on the ground stud.

To characterize the surfaces, 2D height images were created using laser confocal microscopy, and surface roughness parameters were determined according to ISO 4287. A confocal laser scanning microscope (LEXT OLS 4100 from Olympus) was used to perform non-contact roughness measurements and analyze the surface topography. Fig. 5 shows representative electrical contact surfaces of the ground stud and the associated steel cap nut, presented as a real image and 2D height image, including height distribution. The results for the ground stud’s contact surface indicate that the surface topography is predominantly radial. Starting from the center of the stud, the height decreases towards the edges. A slight defect was detected on the surface of the nut. The average roughness depth (Rz) was determined to be 20.7 μm for the ground stud and 14.4 μm for the steel cap nut.

Welding equipment and procedure

For the welding of aluminum ground studs, the arc stud welding system from Stanley Engineered Fastening Tucker GmbH, shown in Fig. 6(a), was used in this study. The control and power unit provides a welding current range from 100 A to 1500 A in both DC and AC forms. The welding head used is equipped with a shielding gas supply and a gas nozzle. The welding table has a 40 mm hollow support, to perform the welds without a backing, as shown in Fig. 6(b).

The welding of aluminum studs is carried out using the AC process. The essential welding parameters for aluminum applications are welding current, welding time, lift height, number of pulses, and polarity (Reis and Braun, 2024). The multiple polarity changes break up the oxide layer on the stud flange and sheet. During the welding process, the welding flange of the ground stud and the workpiece are melted by the arc and cohesively joined by applying relatively low force (approx. 100 N). Additionally, the parameterization of the individual positive and negative pulses allows for targeted heat input into the joining partners. Using a preliminary cleaning phase, adhering residues such as dry lubricants can be removed before the main welding phase. The welding parameters used for the quality-compliant production of the ground stud joints are shown in Table 5. These were determined based on previous investigations. The welds were performed with a preliminary cleaning phase at 100 A for 12 ms to remove local residues on the surface (dry lubricants). The main welding phase lasts a total of 101 ms and is divided into nine individual pulses with alternating polarities. Typically, welding is performed with negative polarity on the stud and positive polarity on the sheet. The preliminary cleaning phase ensures a clean surface for optimal welding conditions, while the alternating polarities help in breaking the oxide layer, ensuring a stronger weld.

The evaluation of the weld connections was carried out using metallographic sections and a torsion test to ensure sufficient mechanical joint strength. Fig. 7 shows an exemplary metallographic section of a produced aluminum weld joint.

A defined sample geometry (70 mm x 250 mm) was used to produce

Table 1
Chemical composition (% by weight) of AlMg3 according to [DIN EN 573–3].

Si	Fe	Cu	Mn	Mg	Cr	Zn	Ti	Notes
0.4	0.4	0.1	0.5	2.6 – 3.6	0.3	0.2	0.15	0.1 – 0.6 Mn+Cr

Table 2
Mechanical properties of AlMg3 according to [DIN EN 485–2].

Material condition	Nominal thickness in mm	Tensile Strength R_m in MPa	Yield point $R_{p0.2}$ in MPa	Elongation at break $A_{50\ mm}$ min. in %	Brinell Hardness HB
O/H111	1.5 – 3.0	190 – 240	80	16	52

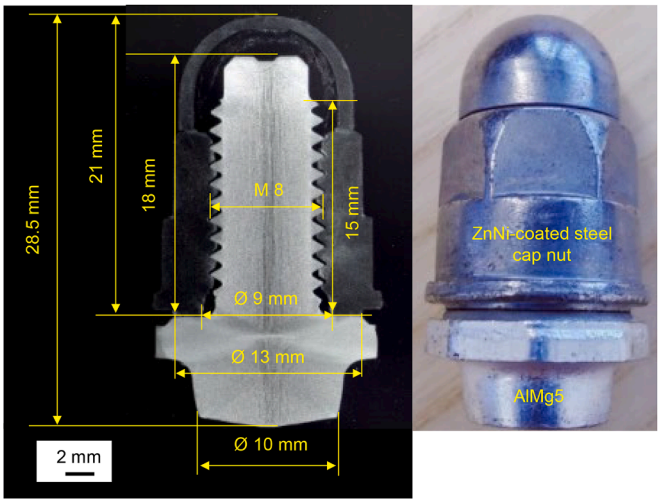

Fig. 3. Geometric characteristics of the ground stud.

Table 3
Chemical composition (% by weight) of AlMg5 according to [DIN EN 573–3].

Si	Fe	Cu	Mn	Mg	Cr	Zn	Ti	Notes
0.4	0.5	0.1	0.1 – 0.6	4.5 – 5.6	0.2	0.2	0.2	0.1 – 0.6 Mn+Cr

Table 4
Mechanical properties of AlMg5 according to [DIN EN 1301–2].

Material condition	Diameter d in mm (up to and including)	Tensile strength R_m in MPa		Yield point $R_{p0.2}$ in MPa	Elongation at break $A_{100\ mm}$ in %
		min.	max.		
H32	18	280	340	205	11

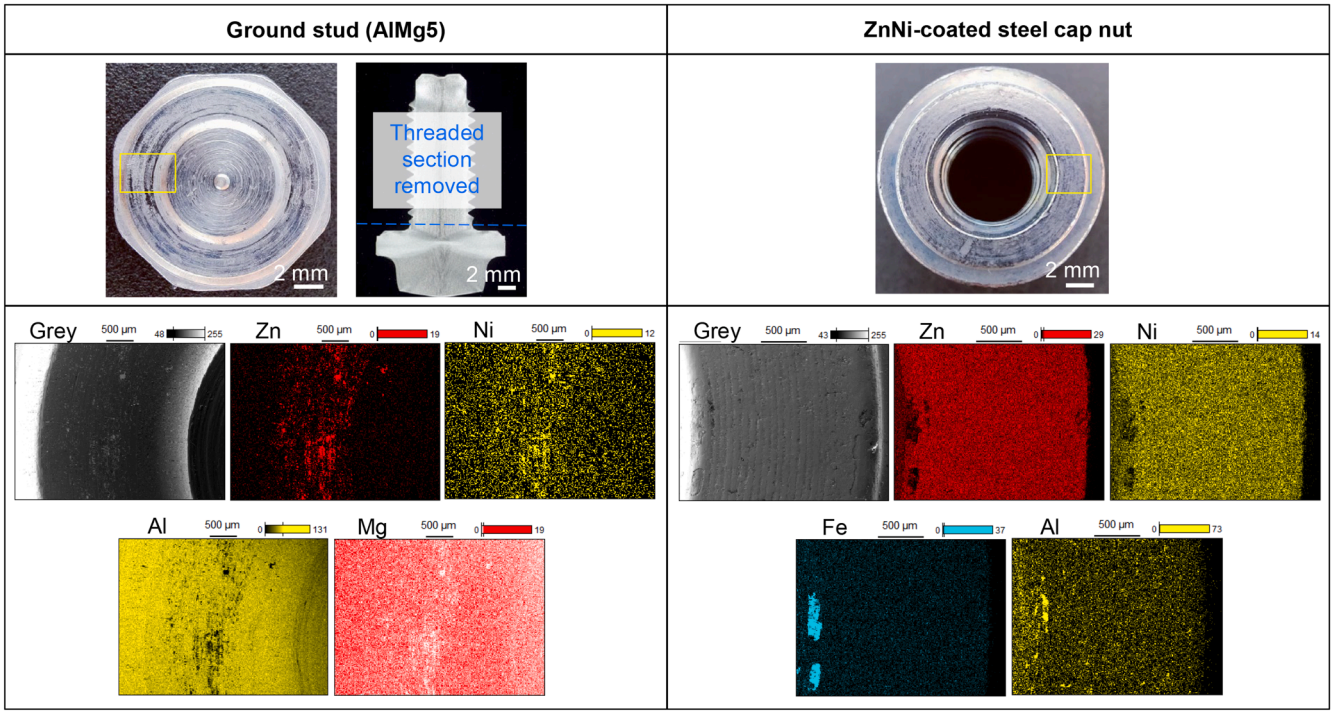

Fig. 4. Overview image (top) and local EDX analysis of the electrical contact surface (bottom) for the aluminum ground stud (left) and the ZnNi-coated steel cap nut (right).

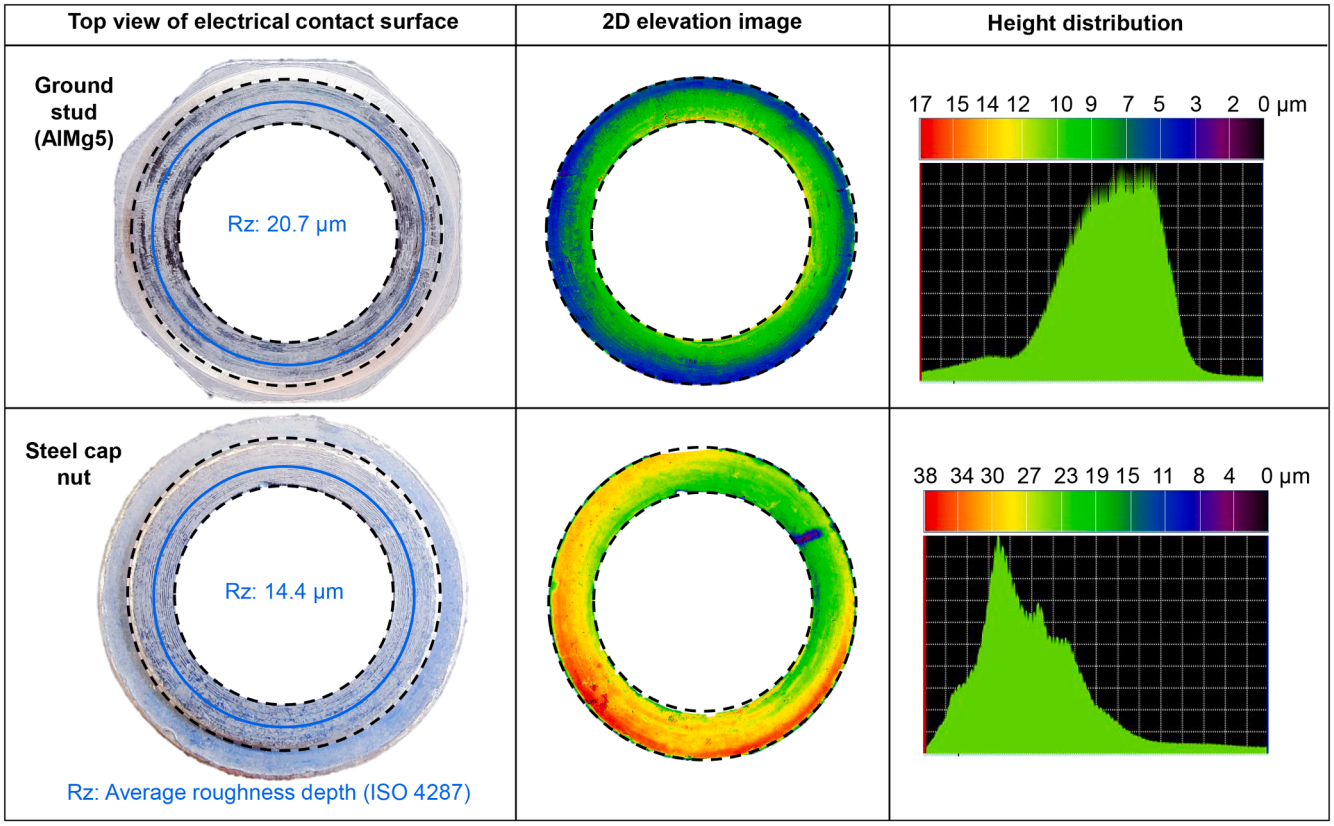

Fig. 5. Top view of the electrical contact surface (left), 2D elevation image (center), and height distribution (right) for the electrical contact surface of the ground stud (top row) and the steel cap nut (bottom row).

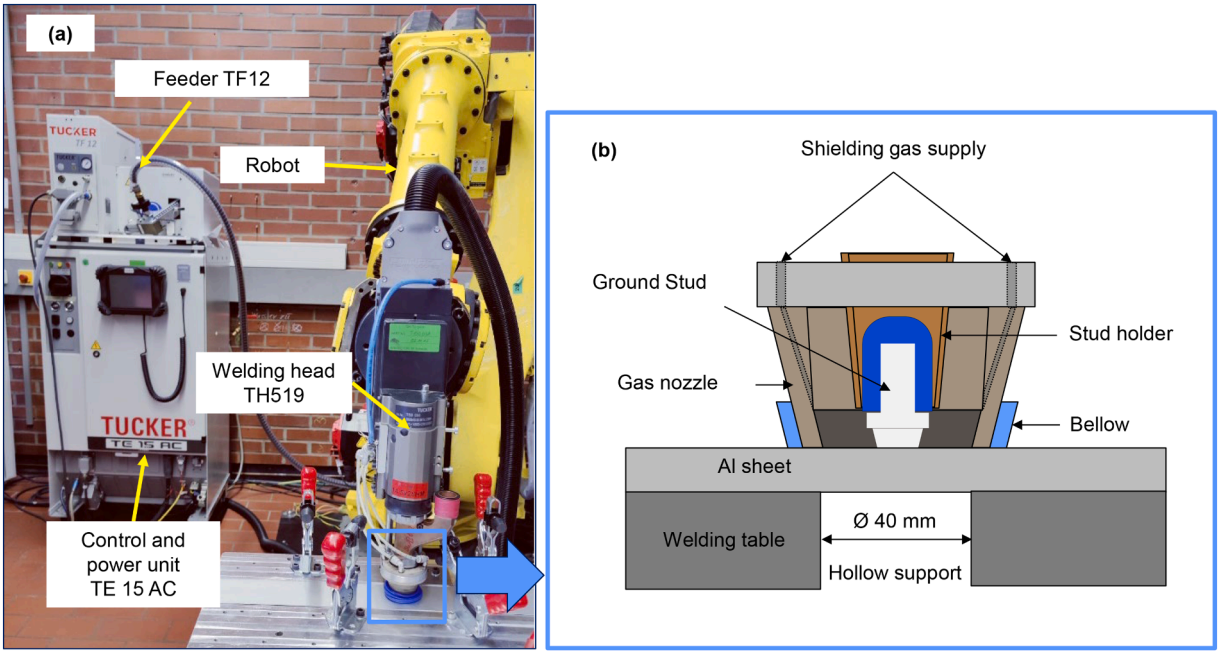

Fig. 6. Welding system (a) and schematic illustration of the setup at the joining position (b).

Table 5
Welding parameters used in the AC process.

	AlMg5 Ground Stud (negative polarity)	AlMg3 Sheet material (positive polarity)
Number of pulses	5	4
Welding time per pulse in ms	13	9
Current in A	−680	+630
Lift height in mm	2.5	2.5
Argon shielding gas volume in L/min	10	10
Penetration in mm	−0.8	−0.8
Drop down time in ms	8	8

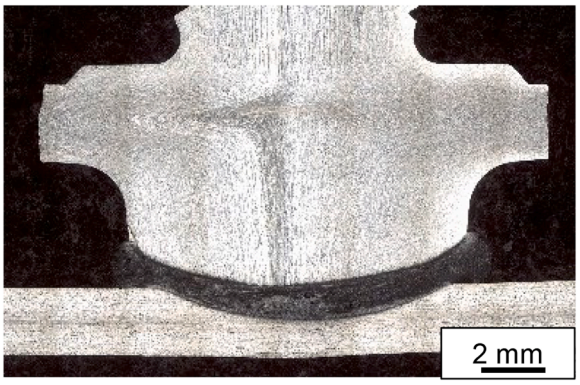

Fig. 7. Metallographic cross-section of the welded ground stud (AlMg5) on sheet material (AlMg3, $t = 2.0$ mm).

the current-carrying test specimens. For this purpose, two ground studs were welded at a distance of 50 mm from the edge and 150 mm from each other (Fig. 8(a)). In the next step, a cable lug was mounted with a specified tightening torque of 9.0 Nm using a digital torque wrench (Fig. 8(b)). A commercially available tubular cable lug made of copper (EN 13600) with an electroplated tin surface and thin-walled automotive cables with PVC insulation (Type FLRY) were used. The automotive cable consists of bare copper strands (CU-ETP1, EN 13602) and has a cross-section of 35 mm^2. The crimping of the cable lugs with the automotive cables was carried out in the form of indent crimping using a press tool provided by the manufacturer. During cable manufacturing, care was taken to ensure that the crimping of the cable lugs was of consistent quality. Fig. 9 (top row of images) presents detailed images of the crimping tool, a crimped cable lug with double-notch crimping, and an exemplary cross-section of a notch crimp. The measured resistances of the assembled cables range from 208.1 to 212.6 μΩ (see diagram in Fig. 9).

Test setup and measuring method

To perform an accelerated test under superimposed load and analyze the electrical long-term stability, a corresponding test setup was realized (Fig. 10). In this setup, the specimens are tested under electrical load in a medial/corrosive environment. For this purpose, a composite of five sheets, each with two welded ground studs in a serial circuit arrangement, was set up inside a climate change chamber. The climate chamber model SKB 1000 A-TR from Liebisch was used to perform the environmental/corrosive load testing. 300 mm long automotive cables were used between the individual test studs. For power supply, two 35 mm^2 cables were used for each. To prevent the ingress of moisture, a heat shrink tube with inner adhesive was additionally used in each crimp connection area. The setup in the test chamber was arranged with an inclination of approximately 10°, allowing condensation to drain off the samples and preventing any influence from standing water. The measurement data (temperature and voltage) at the individual test studs were recorded and monitored using a control and monitoring interface programmed with LabVIEW. This system allows precise data collection and analysis, ensuring the reliability of the test results. With continuous data acquisition, the resistance-time profile can be analyzed and the curve can be described using a mathematical function. This allows for a basic evaluation of the electrical connection quality of the ground stud system and a statement about its long-term stability.

The measurement setup for continuous data acquisition is illustrated in Fig. 11(a) and (b). The temperature at the cable lug is measured using a thermocouple (type K), while the potential difference (voltage tap) and the resulting contact resistance of the respective test stud are measured

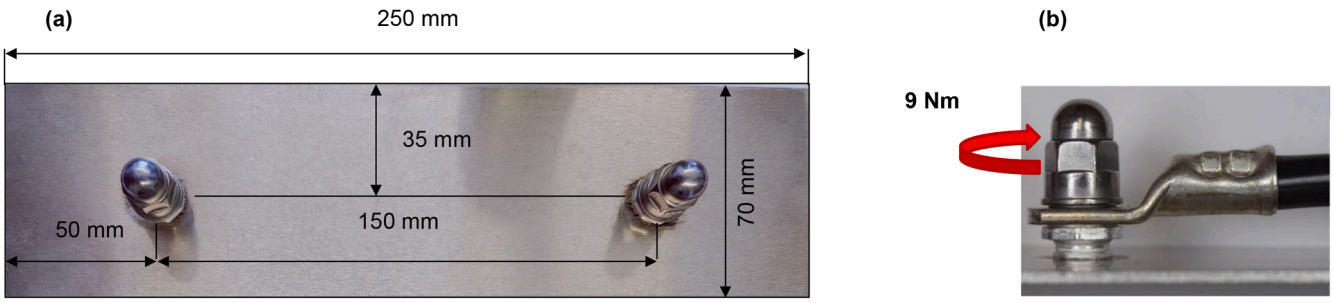

Fig. 8. Specimen geometry with welded ground studs (a), and cable lug mounted with 9.0 Nm tightening torque (b).

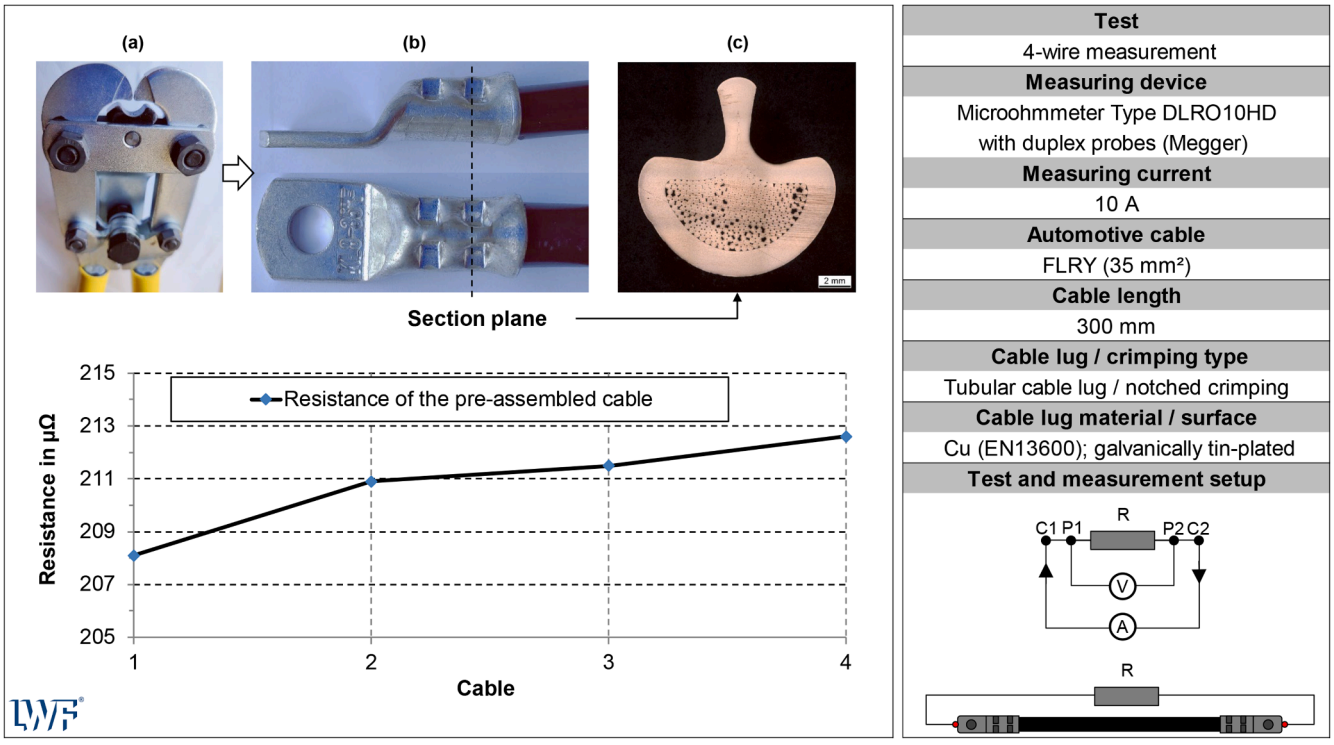

Fig. 9. Crimping tool (a), crimped cable lug (b), exemplary micrograph of a notch crimp (c), and measured resistances of the pre-assembled cables (bottom).

according to the four-wire measurement method. The tolerance and limiting deviation for thermocouples are defined in the DIN EN 60584 standard as ±1.5 °C or 0.40 % for type K thermocouples. The thermocouples were attached with thermostable cable ties, ensuring good contact with the cable lug surface throughout the test period. Fig. 11(c) shows the condition of the thermocouples after 6 weeks of corrosion testing. The area under the cable tie, where the thermocouples were in contact with the cable lug surface, shows no significant corrosive damage. The measurement leads for the voltage tap are each soldered to a copper wire, which is mechanically crimped at the end face of the cable lug and at a distance of 20 mm from the centre of the stud in the aluminum sheet. The defined continuous current of 100 A functions as the test current during the voltage measurement. These methods are crucial for obtaining reliable data on the performance of the ground stud connections under test conditions. With the known quantities of voltage and current, the resistance can be calculated using Ohm's law.

Current load and corrosive test conditions

In real driving conditions, various superimposed loads occur, including electrical-thermal loads from flowing currents, mechanical loads from driving maneuvers and vibrations, and environmental influences. These stresses are characterized by complex processes and interactions arising from manufacturing and material-related factors, as well as a variety of operational and environmental influences. The superimposed loading and associated aging mechanisms create a highly complex condition that leads to an increase in the connection resistance of a ground stud system over its operating lifetime (several years) and therefore, cannot be precisely reproduced by a single test. This study does not aim to exactly reproduce a real test environment but rather to develop a methodical approach and implement a test setup to evaluate the long-term stability of a ground stud system within a short test period. For this purpose, an approach was chosen that considers two key influencing factors of a ground stud system: the electrical-thermal load and the medial/corrosive load. The primary objective of this load configuration (cyclic current profile combined with changing climatic conditions) was to induce accelerated aging within an acceptable test duration (time-lapse test) to ensure the safety and reliability of a ground stud system under extreme environmental and operational conditions and to provide insights into its long-term behavior based on the resistance-time curve.

As a load collective, a corrosion alternating test according to PV 1210 test specification was chosen in combination with a cyclic current profile (Fig. 12). The PV 1210 test specification is used by Volkswagen, for

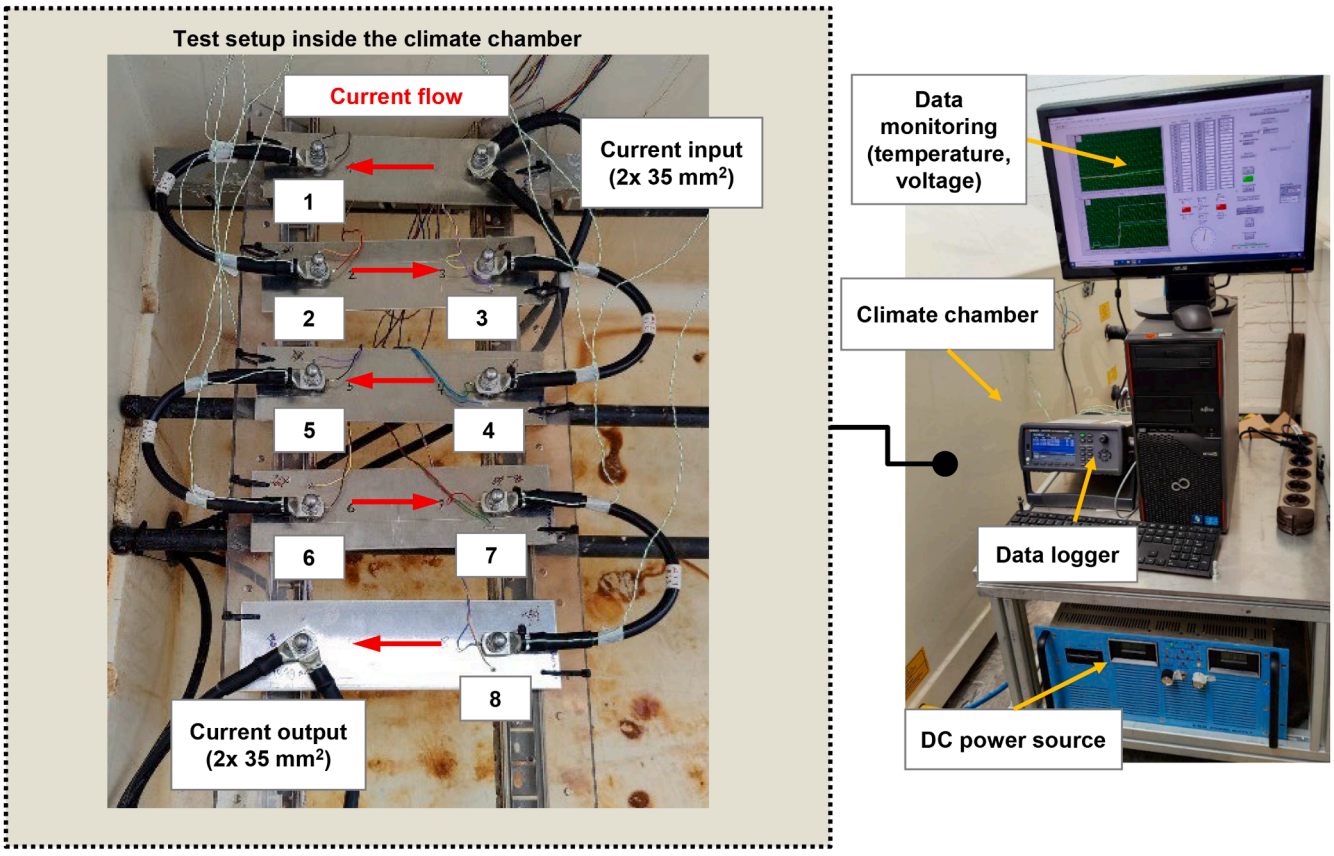

Fig. 10. Test setup for the superimposed load condition.

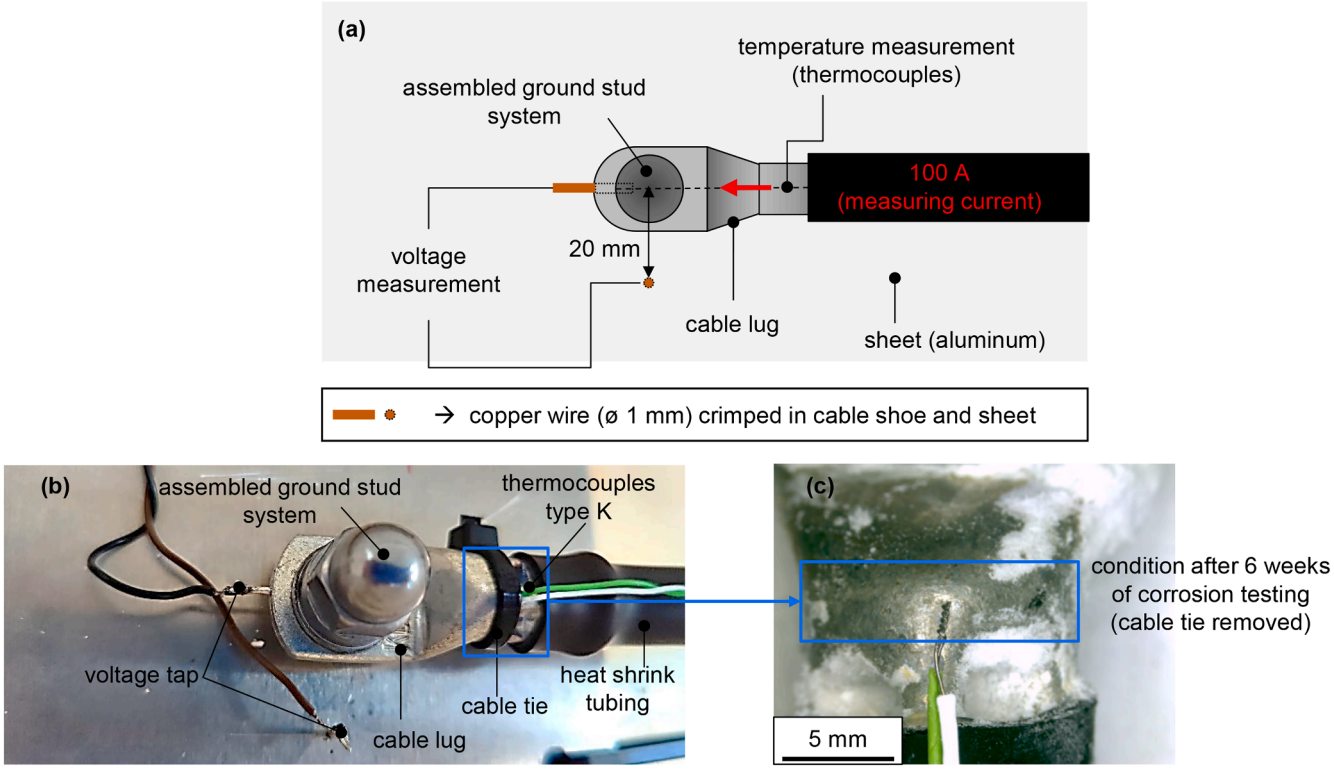

Fig. 11. Schematic measurement setup for continuous measurement data acquisition during the electrical-corrosive load (a), exemplary setup with a real test stud (b), and position of the thermocouples (c).

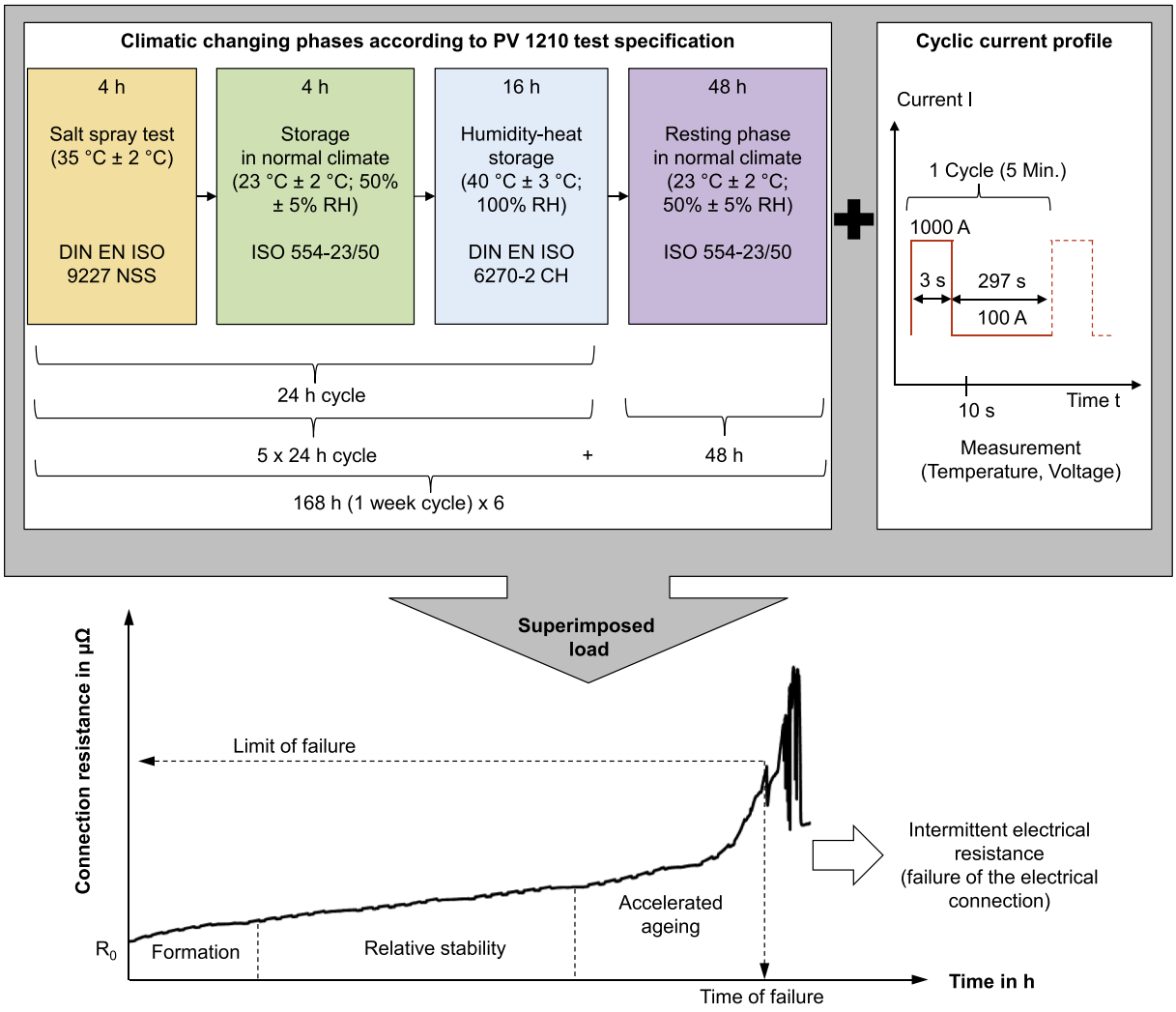

Fig. 12. Electrical-corrosive/medial superimposed load condition (top) and characteristic failure behavior (bottom).

example, to evaluate the corrosion behavior of painted body components with different corrosion protection coatings. The cyclic climate change test consists of various individual tests (see Fig. 12) to assess corrosion behavior under static exposure to salt, moisture, and temperature. The salt spray test, in accordance with DIN EN ISO 9227 NSS, is a well-known method frequently used to evaluate the corrosion resistance of coatings, such as on fasteners. A pH-neutral (pH 6.5 - 7.2) salt fog (5 % NaCl solution) is generated at 35 °C ± 2 °C for 4 h, causing accelerated corrosion on the samples. This is followed by a 4-hour phase in a normal atmosphere, in accordance with ISO 554–23/50, at 23 °C ± 2 °C and 50 % ± 5 % relative humidity. Subsequently, a 16-hour heat-humidity phase in accordance with DIN EN ISO 6270–2 CH (condensation atmosphere with constant humidity) follows at 40 °C ± 3 °C and 100% relative humidity. This proven method in surface technology is used to evaluate the behavior of coated test specimens in a humid environment. A 24-hour test cycle includes the individual tests described (4 h salt spray, 4 h normal climate, 16 h humid heat). After every five cycles, a 48-hour resting phase in a normal atmosphere, in accordance with ISO 554–23/50, follows. This procedure is repeated six times, resulting in a 6-week test duration. The current profile consists of a peak current load (1000 A for 3 s) and a continuous current load (100 A for 297 s). Thus, one cycle lasts a total of 300 s (5 min). The peak current load represents the high current demand during the vehicle's starting process when the starter motor is activated. This is a short but intense process that imposes the maximum load on the electrical system, with several hundred to a thousand amperes flowing. The continuous current load represents the ongoing flow of current during normal driving. This phase accounts for the power requirements of the vehicle's electrical systems and components, such as lighting, air conditioning, assistance, information applications, and other consumers.

Using continuous data acquisition, the temporal profiles of temperature and voltage (connection resistance) are analyzed. Temperature and voltage measurements are taken 10 s after the start of the peak current load at a test current of 100 A. The measurement interval is 5 min. The ground stud connections are subjected to a total of 12,096 current load cycles over a test period of 1008 h. The current-time ratio in the cyclic current load was chosen so that the resulting connection temperature, in combination with the alternating climatic phases, remains below the defined limit temperature to prevent an undesired, premature failure of one of the series-connected connections and thus an early termination of the test. The permissible limit temperature of 105 °C represents the limiting factor of the ground stud system and corresponds to the temperature resistance of the insulation material of the automotive cable. These rigorous test conditions are essential to simulate and understand the long-term behavior and reliability of the electrical connections under extreme conditions.

Results and discussion

To make a statement about the electrical quality and long-term

behavior of a ground stud system, the measurement of the electrical connection resistance using the four-wire measurement method is recommended as the primary test criterion. This includes considering the ground stud system, consisting of the joined ground stud and the mounted cable lug.

Determination of initial ground stud connection resistance

The characteristics of a reliable connection essentially include high electrical conductivity or low connection resistance, as well as robustness and resistance to mechanical, electrical, and thermal influences, and environmental influences. By determining the initial resistances, differences between the individual connections can be identified. Additionally, a reliable connection must be able to maintain its low resistance over time, even under varying environmental conditions such as humidity, temperature fluctuations, and mechanical vibrations. This ensures consistent performance and reliability. Regular monitoring and maintenance are essential to ensure that these connections continue to meet the required standards and to promptly identify any degradation in performance. The considered ground stud system can be simplified into the subsystems of the joint (welded joint) and the screw connection (Fig. 13).

A separate analysis of the resistances enables the determination of individual resistance components of the total resistance and identification of possible process-related differences (e.g. deviations in connection production, quality, or batch fluctuations). This helps uncover potential weak points and optimization opportunities. The initial resistances of the ground stud connections were validated in advance using precise measurements with a digital microohmmeter (DLRO10HD from Megger) equipped with duplex probes. The measurement is based on the four-wire principle, where two current and two voltage wires are used, minimizing the influence of wire resistance and achieving higher accuracy. Measurements were performed as forward and reverse measurements with a test current of 10 A, a resolution of 0.1 μΩ, and a basic accuracy of ± 0.2% / ± 0.2 μΩ.

Fig. 13 (bottom right) illustrates the measuring arrangement for total resistance. Measuring probe 1 is positioned on the cable lug end face, while measuring probe 2 is positioned on the aluminum sheet 20 mm from the center of the stud. The partial resistance of the welded joint is determined similarly, with measuring probe 2 positioned on the stud (outer octagon). Since changes in the total resistance are triggered by the screwed part, knowledge of the partial resistance of the screwed connection is of great interest. However, due to accessibility restrictions of the duplex probes, direct measurement on an already assembled ground stud connection is not possible. Instead, a simple differential calculation between the total resistance and the partial resistance of the welded joint is used to approximate the partial resistance of the screw connection. Fig. 13 shows the measured total resistance and the partial resistances. It can be seen that the welded joint's partial resistance constitutes the larger portion of the total resistance but maintains an almost constant average value of 18.9 μΩ. In contrast, the partial resistance of the screw connection exhibits noticeable fluctuations.

In the context of this study, the welded joint plays a minor role, as it exhibits constant resistance when properly executed. The screw connection, on the other hand, plays a central role, as it is influenced by external environmental factors and is thus crucial for the temporal development of resistance.

In this study, torque was used as the control variable because the torque-controlled tightening method is the most commonly used tightening method in practice due to its relatively simple technical implementation. The tightening torque transmits a preload force to the connection, thereby compressing the ground stud components (stud, nut, cable lug). With the torque-controlled method, the resulting preload force varies with fluctuating coefficients of friction. Friction-related influences cause significant deviations in the resulting preload force even with high torque repeatability. As a result of the fluctuating preload force and thus the contact force in the electrical contact surfaces, variations in the electrical contact resistances occur because these are related to the number and size of the current-carrying contact surfaces.

The initial resistances measured at the start of the test are shown in Fig. 14. The initial resistances of the ground stud connections in the test setup range from 17.0 μΩ to 27.4 μΩ, with an average of 21.5 μΩ ($n = 8$).

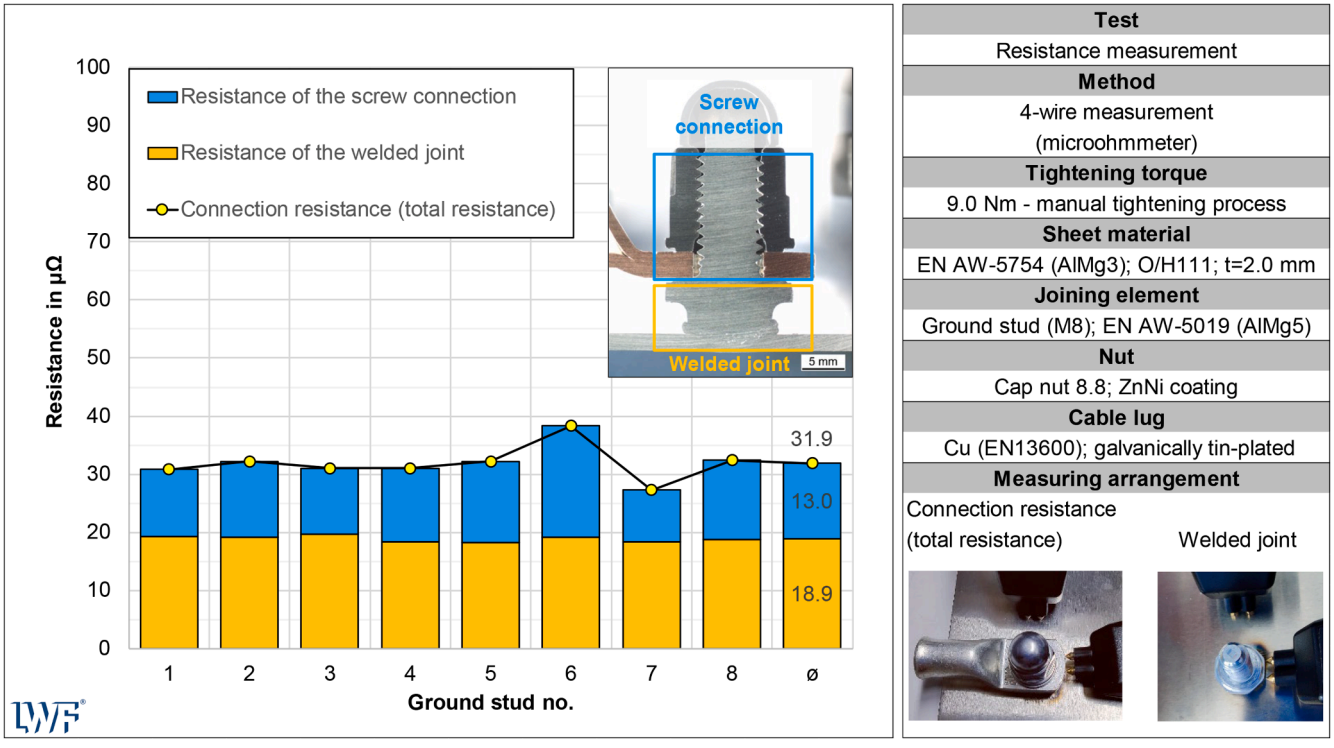

Fig. 13. Subdivision of the ground stud system into the subsystems welded joint and screw connection.

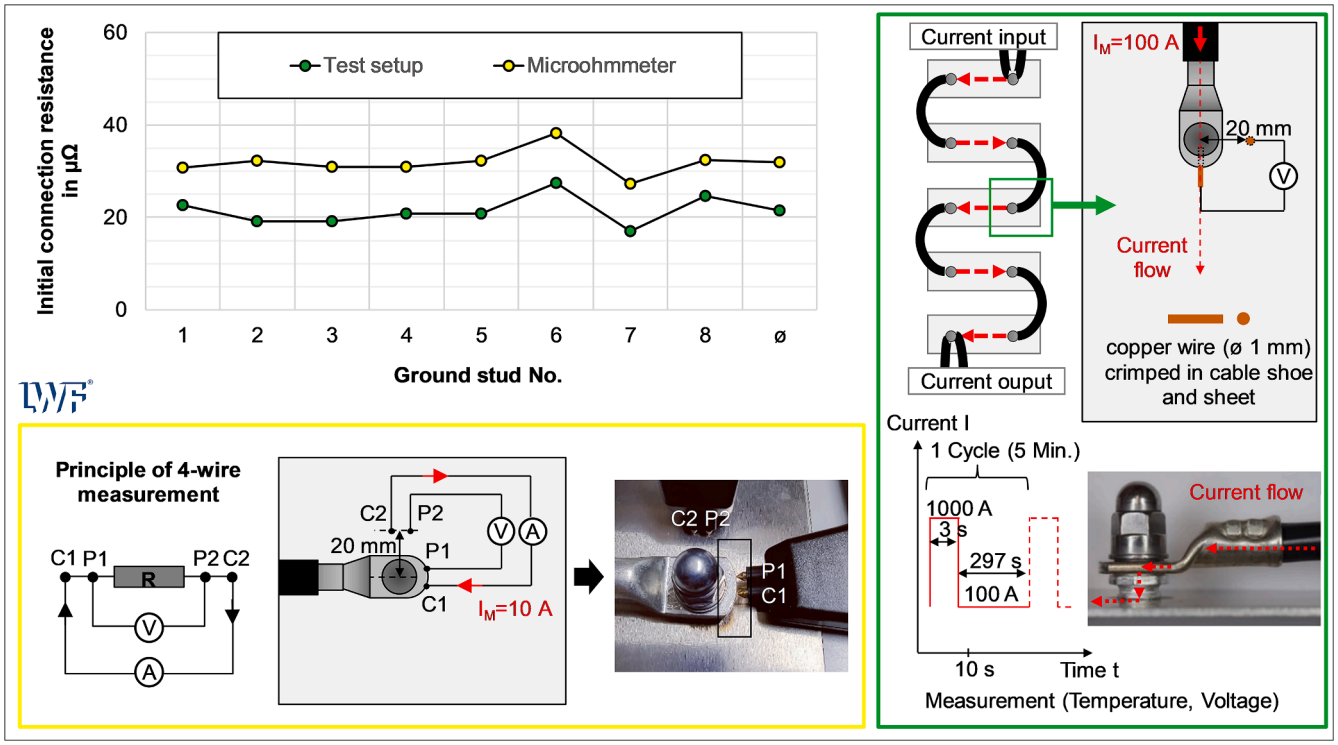

Fig. 14. Determined initial resistance of the ground studs using a microohmmeter and the test setup.

These initial measurements provide a baseline for evaluating changes in electrical connection resistance over the test period. A comparison between the results of the microohmmeter (reference) and the continuous 4-wire measurement in the test chamber shows an average "offset" of approximately 10 µΩ, but comparable resistance ratios are observed (e.g., connection No. 6 highest resistance, connection No. 7 lowest resistance) (Fig. 14). These differences in resistance levels can be explained by different measurement conditions. The microohmmeter measurement was conducted at 10 A with unpowered ground stud connections at room temperature, whereas the continuous resistance measurement in the test setup involved current-loaded ground studs at 100 A, causing heating. At higher temperatures (e.g. due to current

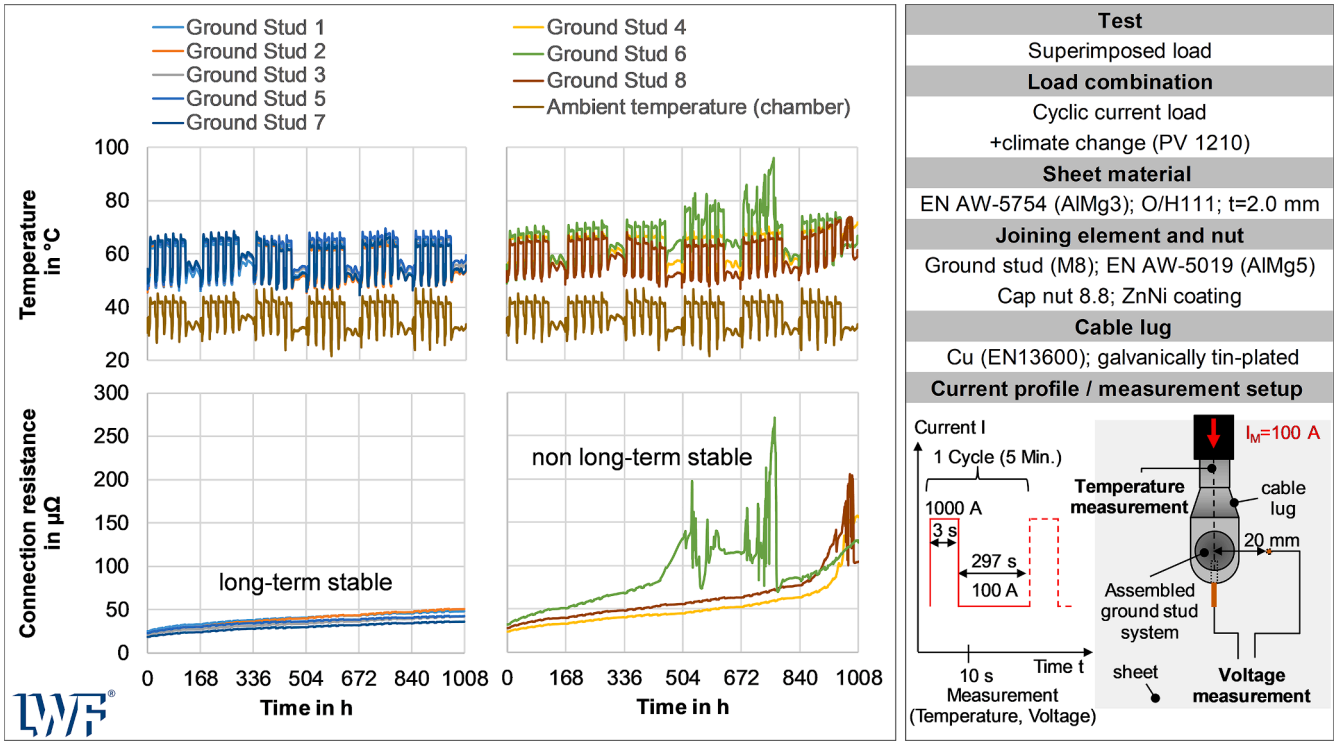

Fig. 15. Temperature-time curve (top), resistance-time curve (bottom) for long-term stable (left) and not long-term stable ground stud connections (right) during the electrical-corrosive/medial superimposed load in the test period of 6 weeks.

flow), the electrical connection points (microcontact surfaces) can behave differently, as the current can force better penetration and utilization of the contact surfaces, leading to a reduction in resistance. The voltage tap with the test setup, positioned outside the current path, eliminates additional resistances that could be detected during a measurement within the current path.

Long-term behavior of ground studs

Fig. 15 shows the temperature-time and connection resistance-time profiles of long-term stable and non-long-term stable ground stud connections over the entire test duration of 1008 h. The results indicate that three out of eight ground stud connections exhibit intermittent resistance behavior and have thus reached the end-of-life phase. The detailed analysis shows that connection No. 6 (green curve), which has an initial resistance approximately 20 % higher, exhibits the fastest and greatest increase in resistance over time (Fig. 16). Over a period of 168 h (1 week), the connection resistance of sample No. 6 increased by 18.7 μΩ, representing a 57.9 % rise, reaching a final resistance of 51.0 μΩ. Similarly, sample No. 8 exhibited an increase in resistance by 11.6 μΩ, corresponding to a 41.3 % increase, resulting in a final resistance of 39.7 μΩ.

The driver of the resistance increase was identified as the climatic phase of humidity-heat storage (40 ± 3 °C, relative humidity of 100 %). In these phase sections, the fastest increase in resistance is observed. This suggests that the combination of temperature and humidity significantly accelerates the degradation process of the electrical contacts. The peak temperatures at the connections are reached in the initial phase of the humid heat storage and, for the majority of the connections, remain below 70 °C during this test period. For connection No. 6, the temperature is already slightly above 70 °C on the third day (72 h). The salt spray and normal climate phases show no significant influence on the contact resistance during the 4-hour intervals. During the two-day climatic rest phase (120 to 168 h), the electrical connections show only a marginal increase in resistance. Using the example of humid heat storage (target temperature of 40 °C ± 3 °C), the measured ambient temperature in the test chamber is slightly higher than 40 °C (Figs. 16–18). The marginally higher values result from residual heat caused by the current load on the ground studs. It can therefore be assumed that the temperature measurement is sufficiently precise and reliable. The temperature curves indicate a system-related transition period between individual phases during which the climatic environment must stabilize. During the normal climate phases, a significantly higher ambient temperature is observed in the test chamber, which is attributed to room air circulation (environment outside the test chamber). Based on the results of the first week, it can be concluded that there is a formation phase during which the electrical connections exhibit a rapid increase in resistance due to the superimposed load in the form of cyclic current loading under varying climatic conditions.

In the further course, the superimposed load leads to a rapid increase in electrical connection resistance, which is accompanied by an increase in thermal power loss, resulting in a higher temperature at the ground stud connection (Fig. 17). Connection No. 6 (green curve) shows accelerated aging from about 408 h onwards. From 336 to 504 h, the contact resistance increases by 90.7 % (about 130 μΩ), which corresponds to an increasing connection temperature. Following the accelerated aging (from 504 h), connection No. 6 exhibits intermittent resistance behavior, characterized by phases of low and high contact resistance. A maximum resistance of almost 200 μΩ is recorded. The intermittent behavior occurs for about 120 h under alternating climatic conditions. This suggests that, under this load, the number and size of the current-carrying microcontacts in the contact zones vary significantly. It is known from power engineering that, in this case, the melting temperature at the microcontacts is reached (Schlegel et al., 2022; Bergmann, 1996). These fluctuations in contact resistance are crucial as they impact the overall performance and reliability of the electrical connections, highlighting the importance of stable resistance profiles for long-term functionality. During the subsequent 48-h climatic rest phase, the contact resistance stabilizes at about 115 μΩ. The observed intermittent resistance behavior is also reflected in the temperature behavior.

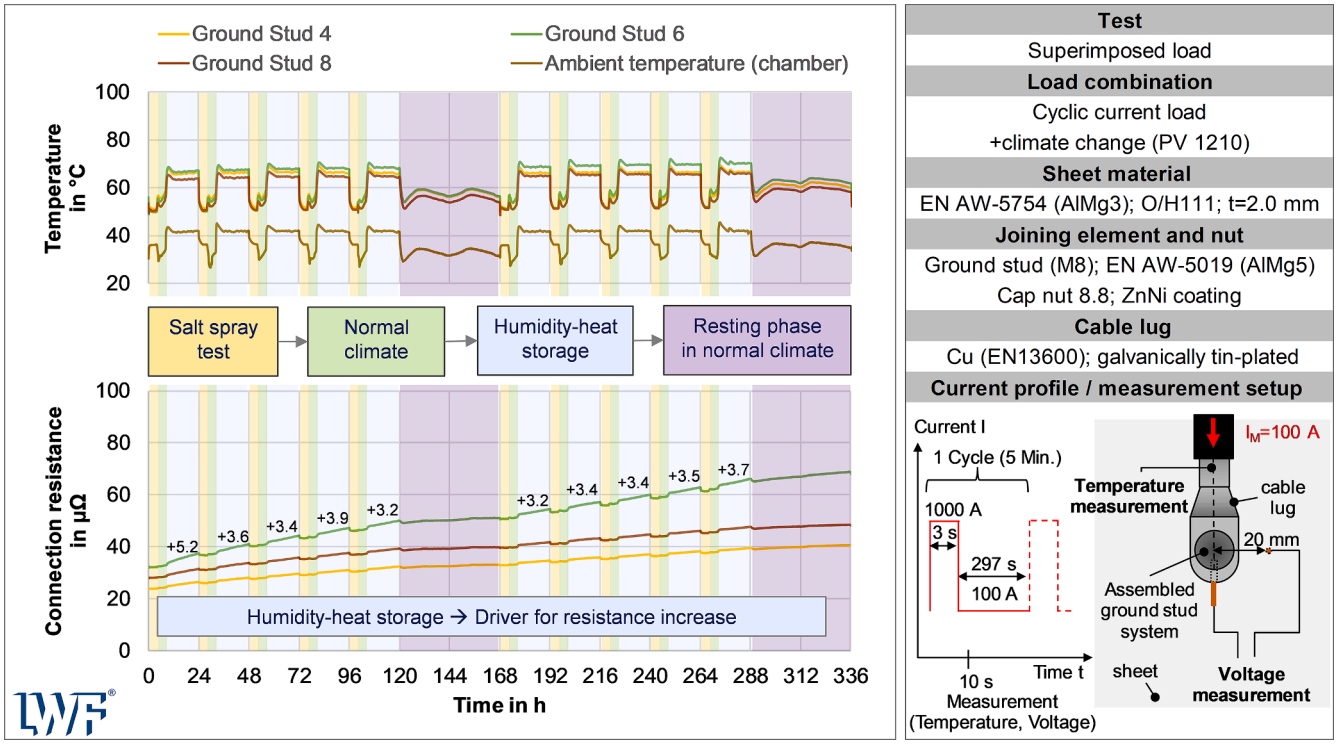

Fig. 16. Temperature-time curve (top), connection resistance-time curve (bottom) during the electrical-corrosive/medial superimposed load in the test period from beginning to 336 h

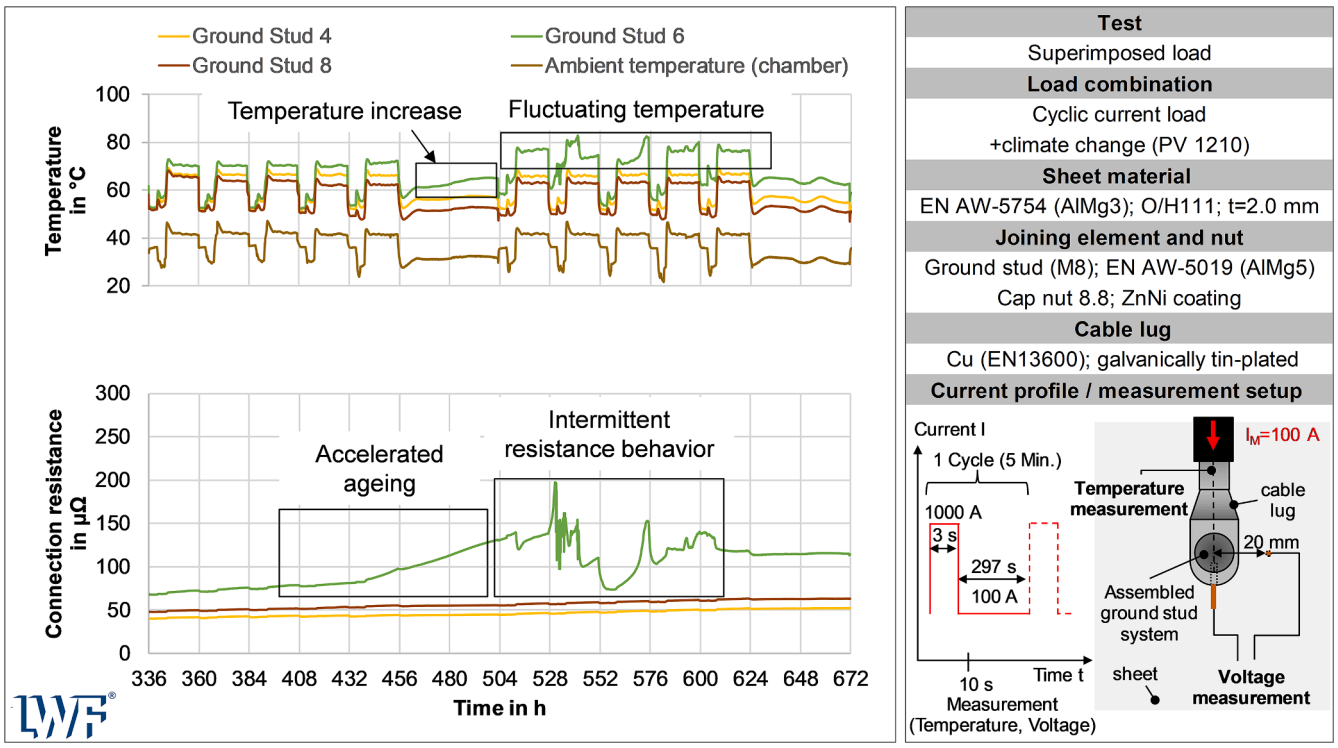

Fig. 17. Temperature-time curve (top), accelerated aging and intermittent connection resistance behavior (bottom) during the test period from 336 h to 672 h

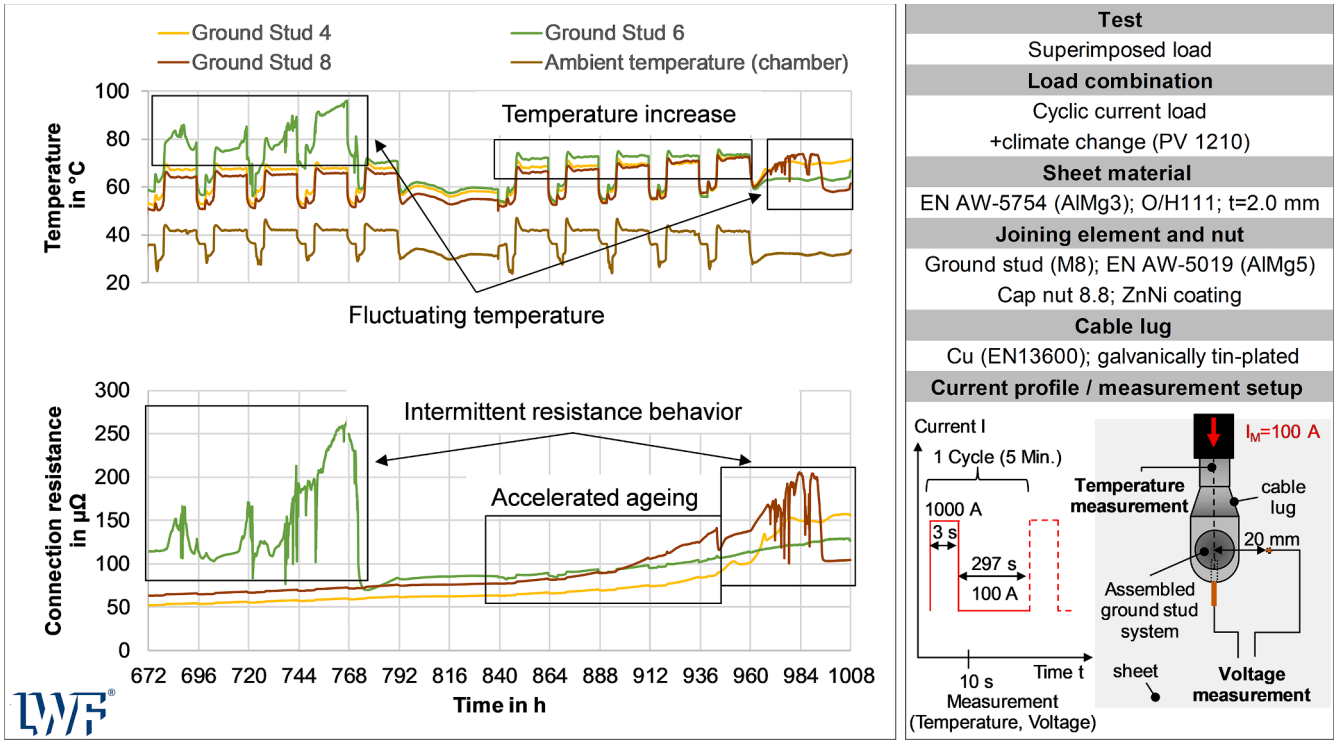

Fig. 18. Temperature-time curve (top), accelerated aging and intermittent connection resistance behavior (bottom) during the test period from 672 h to 1008 h

The other two connections, while exhibiting slightly different resistance levels during this test period, still show a stable contact resistance profile.

In the final third of the test period (672 to 1008 h), connection No. 6 (green curve) continues to show intermittent resistance behavior, with a peak resistance value of nearly 270 µΩ (Fig. 18). The maximum temperature here is about 96 °C, which is close to the defined limit temperature of 105 °C for this system. The resistance and temperature profiles are directly correlated. During the two-day rest phase (792 to 840 h), a constant contact resistance of about 85 µΩ is observed. Toward the end of the test period, an increasing resistance trend without intermittence is observed. During the test period from 840 to 1008 h,

connections No. 4 (yellow curve) and No. 8 (brown curve) also exhibit accelerated aging followed by intermittent resistance behavior. The fluctuations (minimum and maximum) observed for connection No. 4 (yellow curve) are less pronounced compared to the other connections. These findings highlight the variability in long-term performance among the tested connections and underscore the importance of reliable contact resistance for the longevity of ground stud connections. It can be concluded that the initial connection resistance has a significant impact on the resistance development and thus substantially influences the timing of the electrical failure of the ground stud connections.

Damage analysis

The damage analysis of the components of unstable connections is illustrated in Fig. 19. This figure provides a detailed examination of three different ground stud systems, each exhibiting varying levels of resistance and associated damage. The images reveal significant media penetration into the electrical contact zones, specifically between the nut and cable lug, as well as between the cable lug and stud. This penetration results in the formation of local corrosive products and deposits within the electrical contact zones. The presence of these corrosive elements adversely affects the number and size of microcontact areas, leading to a marked increase in resistance and ultimately resulting in intermittent resistance behavior. In greater detail, the assembled ground stud connection No. 6, with an initial resistance of 27.4 μΩ, shows substantial degradation. The images depict the top side of the cable lug, ground stud, and the underside of the cable lug, highlighting areas where media penetration has occurred. The corrosive deposits are clearly visible, indicating significant deterioration of the contact surfaces. This degradation reduces the effectiveness of the electrical connection, as evidenced by the high resistance value. Ground stud connection No. 8, with an initial resistance of 24.7 μΩ, also demonstrates considerable damage. The cap nut shows clear signs of media ingress, with the arrows indicating areas of concentrated corrosive activity. The ground stud and cable lug surfaces are similarly affected, with visible corrosion and deposit buildup. These defects are critical, as they diminish the contact force, reducing the number of effective microcontact areas and thereby increasing the overall resistance. Ground stud connection No. 4, with the lowest initial resistance of 20.8 μΩ, shows less severe but still significant damage. The images reveal localized areas of media penetration and corrosion, particularly around the cable lug and ground stud interface. Although less extensive than in the other systems, these areas of damage still contribute to increased resistance and potential connection instability. The analysis underscores the crucial impact of media penetration and the subsequent formation of corrosive products on the long-term reliability of electrical connections. The presence of corrosion not only increases resistance but also promotes intermittent resistance behavior, which can lead to connection failures. These findings highlight the importance of understanding and mitigating the effects of environmental factors on ground stud systems to ensure their durability and reliability in automotive applications.

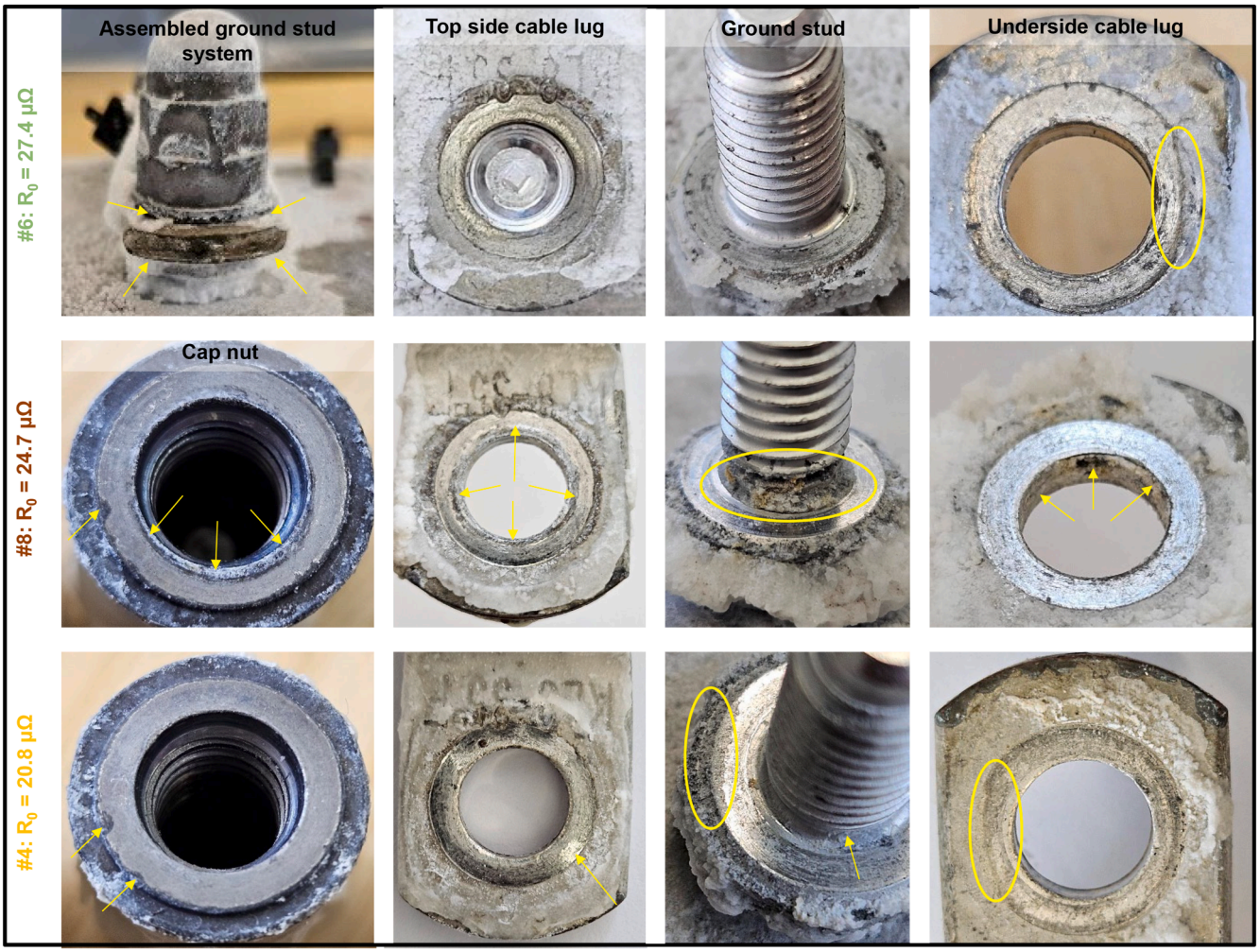

Fig. 19. Damage analysis of the individual components on ground bolt connections.

Prediction of long-term behavior based on the resistance-time curve

At this point, it can be stated that in the course of these investigations, three out of eight ground stud connections have reached the end-of-life phase, in which reliable electrical function is no longer ensured. The findings highlight that, in addition to the resistance level, understanding the temporal progression with the individual lifespan phases is of great importance. For a ground stud system measured in practical applications, knowing the lifespan phase of the ground stud at any given time is highly advantageous. Otherwise, incorrect assumptions may be made, such as when a low resistance is measured during an intermittent phase. This can lead to the false conclusion that it is a seemingly "acceptable connection," even though it is already exhibiting intermittent resistance behavior and can no longer reliably ensure electrical function. In the detailed analysis, a characteristic resistance drop can be observed in the resistance profile of the unstable connections shortly before the beginning of the intermittent phase (Fig. 20). This characteristic is due to the attainment of the melting temperature in the current-carrying microcontacts. This point in the resistance profile can therefore be taken as an indicator of the failure time. The occurrence of this resistance drop signifies that the electrical connection has reached a critical thermal threshold, leading to degradation. Based on this point, a qualification criterion or the limit of the connection resistance ($R < x$) for a long-term stable ground stud system can be estimated for the considered test conditions. The following failure times can thus be determined for the three connections:

- 512 h: Connection No. 6 (green curve)
- 944 h: Connection No. 8 (brown curve)
- 966 h: Connection No. 4 (yellow curve)

The long-term behavior and the limit for long-term stability - under the operating and environmental conditions carried out here - can be described for the ground stud system on the basis of the underlying data. Based on the profiles of five stable ground stud connections, the resistance-time profile can be described with a linear function of the form $y = 0.0192x + 26.357$ (Fig. 21, purple curve). The coefficient of determination is 0.9617. After 1008 h, the stable ground stud connections are in the phase of relative stability with an average value of 44 μΩ (+6.8 μΩ and −7.7 μΩ). For the unstable ground stud connections, the resistance-time curve up to the time of failure can be described very well using exponential functions (green, brown and yellow curve). In this case, the coefficient of determination is in the range from 0.9488 to 0.9554. Up to the time of failure, a connection resistance of 135 μΩ is determined for connection No. 4 and a slightly higher value of approx. 140 μΩ for connection No. 6 and No. 8. The use of linear and exponential functions to describe the resistance-time profiles is crucial for accurately predicting the performance and lifespan of the ground stud connections under various conditions.

Conclusions and outlook

In this study, an experimental and testing methodology was developed that enables a fundamental assessment of the electrical connection quality of a ground stud system, as well as an evaluation of long-term stability under superimposed electrical-medial/corrosive load. This methodology is crucial for understanding the performance and durability of ground stud connections in automotive applications. The main results are as follows:

(1) The realized measurement and testing setup allows the analysis of the long-term electrical behavior of ground stud systems based on the continuous resistance and temperature-time profiles.
(2) The chosen operational and environmental conditions in the form of a cyclic current profile under varying climatic phases enable accelerated aging and the subsequent failure of the electrical connections within the test period of 1008 h.
(3) The results show that three out of eight ground stud connections have reached the end-of-life phase (intermittent resistance behavior), where reliable electrical function can no longer be ensured.

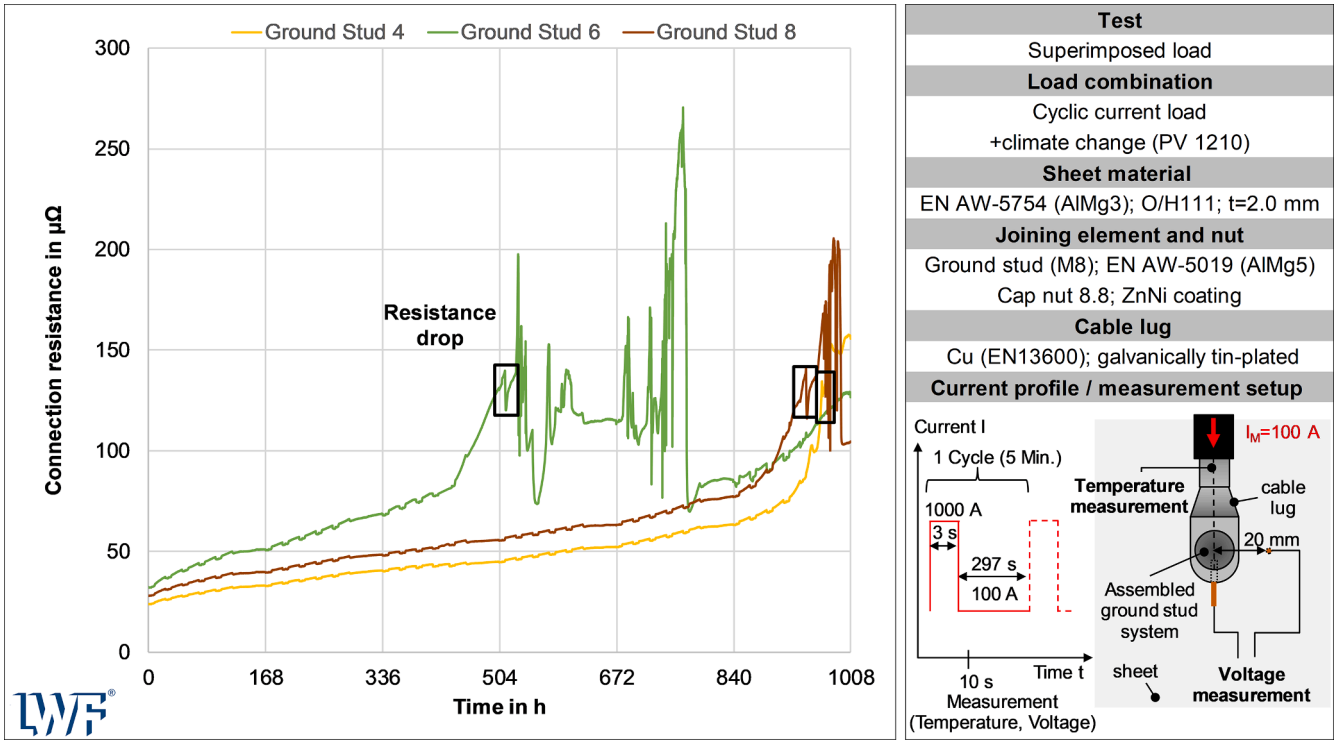

Fig. 20. Connection resistance-time curve with characteristic drop in resistance shortly before the start of the intermittent phase.

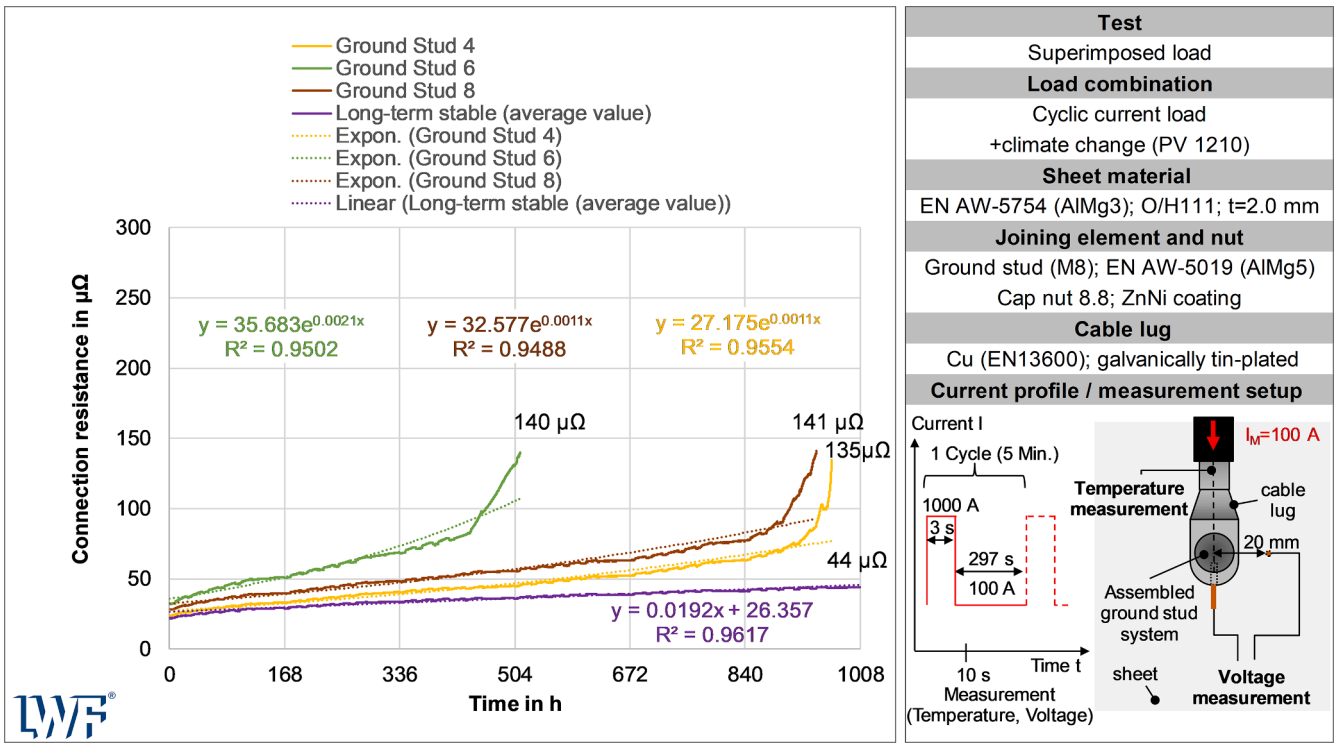

Fig. 21. Resistance-time curve of the long-term stable and unstable connections as well as the critical limits reached with the electrical-medial/corrosive superimposed load.

(4) The humidity-heat storage phase (40 ± 3 °C; 100 % humidity) was identified as the driver for the resistance increase.
(5) The initial resistance of the examined ground stud system is a significant factor influencing electrical long-term stability under the selected operating and environmental conditions. An increased initial resistance of about 20 % leads in this case to an early electrical failure of the ground stud connections after about 512 h.
(6) In the resistance-time profile, a characteristic point before the first resistance drop can be determined. This serves as an indicator for the imminent intermittence of the ground stud system as well as a specific failure time and critical resistance limit.
(7) The generated lifetime curve enables the analysis and assessment of long-term behavior. A good description of the long-term behavior for the unstable ground stud connections was shown using an exponential function up to the point of initial failure with a coefficient of determination of R^2=0.95.

This research makes a notable contribution to the field by deepening the understanding of ground stud system performance in challenging conditions, thereby facilitating the development of more robust and reliable connections. It provides valuable insights for both users and manufacturers on the economical production and assessment of long-term stable ground stud connections in automotive contexts.

A ground stud system is more robust and resistant to external influences, such as corrosion and media infiltration, if the number and size of the microcontacts are maximized, resulting in comparatively low initial resistance. The following strategies are proposed for manufacturing long-term stable ground stud connections: The surface and material combination of the contact partners is a significant influencing factor. When using different materials (steel nut, aluminum alloy stud, copper cable lug) and different contact surfaces, significant chemical (corrosion) and physical effects (e.g., thermal expansion during temperature changes) can occur due to environmental and operating conditions, influencing the microcontacts and the aging rate. One strategy is to select optimized materials and coatings that behave similarly under different operating and environmental conditions. For example, the nut and bolt could be made of the same base material to reduce thermal effects from temperature changes or corrosion. Increasing effective contact surfaces can also help reduce resistance. This can be achieved by using components with optimized geometry to maximize the number of current-carrying microcontacts. A modified cable lug design or an adjustment of the stud and/or nut contact surface could further improve contact quality. The nut tightening process (tightening torque method, screwing parameters) is another decisive factor affecting initial resistance and contributes significantly to the long-term stability of the ground stud connection. The contact force generated by tightening significantly affects the current-carrying microcontact surfaces at the two contact levels (nut-cable lug and cable lug-stud). Fluctuating friction values (thread and underhead friction) of the ground stud components (nut, stud, cable lug) can lead to fluctuating contact forces with the torque-based tightening method, even when the correct tightening torque is applied. This can significantly affect the initial resistance of the screw connection and influence resistance to media penetration. Manufacturers and users should consider possible deviations in friction ratios to minimize variations in contact force and ensure the long-term electrical stability of the screw connection. One possible fastening approach is a combination of torque- and angle-controlled methods (up to the plastic range), which reduces fluctuations in preload force caused by variable friction values and ensures a consistent and sufficiently high contact force for a reliable electrical connection.

Consequently, future research should investigate the impact of tightening torques and the resultant preload force on ground stud connections, as the contact force greatly influences the current-carrying microcontact areas, initial resistance, and overall service life in automotive applications.

Funding

The research project IGF 21908 N "Investigation of superimposed loads on the electrical connection properties of thermally and form-joined ground studs on modern aluminum materials" was supported by the Federal Ministry of Economic Affairs and Climate Action through as part of the program for promoting industrial cooperative research (IGF) on the basis of a decision by the German Bundestag.

CRediT authorship contribution statement

Viktor Haak: Writing – review & editing, Writing – original draft, Methodology, Investigation, Formal analysis, Data curation, Conceptualization. **Keke Yang:** Writing – review & editing, Writing – original draft, Formal analysis, Conceptualization. **Gerson Meschut:** Writing – review & editing, Supervision, Resources, Methodology, Funding acquisition, Conceptualization.

Declaration of competing interest

The authors declare that they have no known competing financial interests or personal relationships that could have appeared to influence the work reported in this paper.

Acknowledgements

The research project IGF 21908 N "Investigation of superimposed loads on the electrical connection properties of thermally and form-joined ground studs on modern aluminum materials" from the Research Association Stifterverband Metalle e.V.,Berlin, was supported by the Federal Ministry of Economic Affairs and Climate Action through as part of the program for promoting industrial cooperative research (IGF) on the basis of a decision by the German Bundestag. The project was carried out at laboratory for materials and joining (LWF), Paderborn University.

Data availability

Data will be made available on request.

References

Bergmann, R., 1996. Dissertation. Technische Universität Dresden, Fortschritt-Berichte VDI Nr. 195.

Braunovic, M., 1981. Effect of current cycling on contact resistance, force, and temperature of bolted aluminium-to-aluminium connectors of high ampacity. IEEE Trans. Compon., Hybrids, Manuf. Technol. 4 (1), 57–69. https://doi.org/10.1109/TCHMT.1981.1135772.

Braunovic, M., 2009. Fretting in electrical/electronic connections: a review. IEICE Trans. Electron. E92-C (8), 982–991. https://doi.org/10.1587/transele.E92.C.982.

Czerwinski, F., 2021. Current trends in automotive lightweighting strategies and materials. Materials. (Basel) 14 (21), 6631. https://doi.org/10.3390/ma14216631.

Emadi, P., Bernoulli, A., Ravindran, C., 2022. Engineering lightweight aluminum and magnesium alloys for a sustainable future. J. Indian Inst. Sci. 102 (1), 405–420. https://doi.org/10.1007/s41745-021-00267-9.

Füssel, U., Schlegel, S., Reschke, G., Kalich, J., 2022. Electrical contacting of aluminum bus bars using clinching and functional elements. In: Paper presented at the SFU/ICAFT 2022. MDPI, p. 5. https://doi.org/10.3390/engproc2022026005.

Geng, P., Qin, G., Zhou, J., Li, T., Ma, N., 2021a. Characterization of microstructures and hot-compressive behavior of GH4169 superalloy by kinetics analysis and simulation. J. Mater. Process. Technol. 288, 116879. https://doi.org/10.1016/j.jmatprotec.2020.116879.

Geng, P., Qin, G., Ma, H., Zhou, J., Ma, N., 2021b. Linear friction welding of dissimilar Ni-based superalloys: microstructure evolution and thermo-mechanical interaction. J. Mater. Res. Technol. 11, 633–649. https://doi.org/10.1016/j.jmrt.2021.01.036.

Godard, H.P., 1967. Oxide film growth over five years on some aluminum sheet alloys in air of varying humidity at room temperature. J. Electrochem. Soc. 114 (4), 354. https://doi.org/10.1149/1.2426593.

Hildmann, C., 2017. Dissertation. Technische Universität Dresden.

Hilmert, D., Yuan, H., Song, J., 2022. The analysis of failure mechanisms of electrical connectors in long-term use field vehicles. In: Paper presented at the 2022 IEEE 67th Holm Conference on Electrical Contacts (HLM). IEEE, pp. 1–8. https://doi.org/10.1109/HLM54538.2022.9969820.

Hirsch, J., 2014. Recent development in aluminium for automotive applications. Trans. Nonferrous Met. Soc. China 24 (7), 1995–2002. https://doi.org/10.1016/S1003-6326(14)63305-7.

Hsu, C., 2015. Mechanical Fastening Techniques for Advanced High-Strength Steels (AHSS). Welding and Joining of Advanced High Strength Steels (AHSS). Elsevier, pp. 181–186. https://doi.org/10.1016/B978-0-85709-436-0.00010-2.

Hu, L., Wang, X., Ma, Q., Meng, W., Chen, S., 2021. Numerical and experimental investigations on the temperature field in local post weld heat treatment of 9% Cr heat resistant steel welded pipes. J. Mater. Process. Technol. 297, 117232. https://doi.org/10.1016/j.jmatprotec.2021.117232.

Hunter, M.S., Fowle, P., 1956. Natural and thermally formed oxide films on aluminum. J. Electrochem. Soc. 103 (9), 482. https://doi.org/10.1149/1.2430389.

Kloch, K.T., Kozak, P., Mlyniec, A., 2021. A review and perspectives on predicting the performance and durability of electrical contacts in automotive applications. Eng. Fail. Anal. 121, 105143. https://doi.org/10.1016/j.engfailanal.2020.105143.

Kohler, T.P., Gehring, R., Froeschl, J., Buecherl, D., Herzog, H.G., 2011. Voltage stability analysis of automotive power nets based on modeling and experimental results. New Trends and Developments in Automotive System Engineering. InTech. https://doi.org/10.5772/13127.

Li, H., Liu, X.S., Zhang, Y.S., Ma, M.T., Li, G.Y., Senkara, J., 2019. Current research and challenges in innovative technology of joining dissimilar materials for electric vehicles. In: Paper presented at the 4th International Conference on Advanced High Strength Steel and Press Hardening (ICHSU2018). WORLD SCIENTIFIC, pp. 363–380. https://doi.org/10.1142/9789813277984_0056.

Lumley, R., 2011. Fundamentals of Aluminium Metallurgy: production, Processing and Applications. Woodhead Publishing in Materials. Woodhead Publ.

Oberg, A., Gustafsson, R., Saksvik, O., Stomberg, H., Olsson, K.-E., 1996. The ageing physics of electrical contacts subjected to DC current. Paper presented at the Electrical Contacts - 1996. In: Forty-Second IEEE Holm Conference on Electrical Contacts. Joint with the 18th International Conference on Electrical Contacts. IEEE, pp. 189–194. https://doi.org/10.1109/HOLM.1996.557196.

Ostermann, F., 1998. Physikalische und mechanische Eigenschaften. Anwendungstechnologie Aluminium. Springer Berlin Heidelberg, pp. 77–104. https://doi.org/10.1007/978-3-662-05788-9_4.

Ostermann, F., 2014. Korrosion. Anwendungstechnologie Aluminium. Springer Berlin Heidelberg, pp. 217–270. https://doi.org/10.1007/978-3-662-43807-7_5.

Pan, B., Sun, H., Shang, S.L., Wen, W., Banu, M., Simmer, J.C., Carlson, B.E., Chen, N., Liu, Z.K., Zheng, Z., Wang, P., Li, J., 2021. Corrosion behavior in aluminum/galvanized steel resistance spot welds and self-piercing riveting joints in salt spray environment. J. Manuf. Process. 70, 608–620. https://doi.org/10.1016/j.jmapro.2021.08.052.

Pfeifer, S., 2015. Dissertation. Technische Universität Dresden.

Rachman, N.A., Risdiyanto, A., Khayam, U., Suwarno, 2013. Analysis of surface roughness and contact pressure at copper connector using nickel and silver plating for EV battery. In: Paper presented at the 2013 Joint International Conference on Rural Information & Communication Technology and Electric-Vehicle Technology (rICT & ICeV-T). IEEE, pp. 1–6. https://doi.org/10.1109/rICT-ICeVT.2013.6741527.

Ramasamy, S., 2000. Drawn arc stud welding: crossing over from steel to aluminum. Weld. J. 79 (1).

Ramasamy, S., 2002. Drawn arc aluminum atud welding for automotive applications. JOM 54 (8), 44–46. https://doi.org/10.1007/BF02711866.

Reis, C., Braun, M., 2024. Enhancement and process optimization for drawn arc stud welding. In: Paper presented at Joining in Car Body Engineering. Rochester, MI, United States. February 27-28.

Robinson, A.L., Taub, A.I., Keoleian, G.A., 2019. Fuel efficiency drives the auto industry to reduce vehicle weight. MRS Bull. 44 (12), 920–923. https://doi.org/10.1557/mrs.2019.298.

Sampaio, R.F.V., Pragana, J.P.M., Bragança, I.M.F., Silva, C.M.A., Fernandes, J.C.S., Martins, P.A.F., 2022. Influence of corrosion on the electrical and mechanical performance of hybrid busbars. Int. J. Lightweight Mater. Manuf. 5 (4), 510–519. https://doi.org/10.1016/j.ijlmm.2022.06.005.

Sanguesa, J.A., Torres-Sanz, V., Garrido, P., Martinez, F.J., Marquez-Barja, J.M., 2021. A review on electric vehicles: technologies and challenges. Smart Cities 4 (1), 372–404. https://doi.org/10.3390/smartcities4010022.

Schlegel, S., Gatzsche, M., Hildmann, C., Israel, T., 2022. Kontakt- und Langzeitverhalten Stromführender Verbindungen in Der Elektroenergietechnik: Theorie und Praxis zum Verhalten, Berechnungsansätze sowie Konstruktions- und Auslegekriterien. Springer Berlin Heidelberg. https://doi.org/10.1007/978-3-662-64658-8.

Schlegel, S., Grossmann, S., Lakner, M., Schoenemann, T., 2012. Investigations on material structural changes on electrical joints at high contact temperature. In: Paper presented at the 26th International Conference on Electrical Contacts (ICEC 2012). IET, pp. 7–11. https://doi.org/10.1049/cp.2012.0613.

Schneider, R., Löbl, H., Großmann, S., Schoenemann, T., Holdis, M., 2009. Langzeitverhalten von aluminium-kupfer-verbindungen in der elektroenergietechnik. Metall 63 (11), 591–594.

Scrosati, B., Garche, J., Tillmetz, W., 2015. Advances in Battery Technologies For Electric Vehicles. Elsevier. https://doi.org/10.1016/C2014-0-02665-2.

Song, J., Yuan, H., Koch, C., 2018. Accelerated testing of electromechanical connectors considering thermal and mechanical loads. In: Paper presented at the 2018 IEEE Holm Conference on Electrical Contacts. IEEE, pp. 467–474. https://doi.org/10.1109/HOLM.2018.8611653.

Spahr, M., 2017. Automatisierte Kontaktierungsverfahren für flachleiterbasierte Pkw-Bordnetzsysteme. Dissertation. Friedrich-Alexander-Universität Erlangen-Nürnberg.

Sun, X., Han, X., Dong, C., Li, X., 2021. Applications of Aluminum Alloys in Rail Transportation, Aluminium Alloys. IntechOpen. https://doi.org/10.5772/intechopen.96442.

Taub, A.I., Luo, A.A., 2015. Advanced lightweight materials and manufacturing processes for automotive applications. MRS Bull. 40 (12), 1045–1054. https://doi.org/10.1557/mrs.2015.268.

Vural, M., 2014. Welding Processes and Technologies. Comprehensive Materials Processing. Elsevier, pp. 3–48. https://doi.org/10.1016/B978-0-08-096532-1.00603-8.

Wu, C.T., Ma, N., Guo, Y., Hu, W., Takada, K., Okada, H., Saito, K., 2018. A dynamic ductile failure analysis of shell structures using a nonlocal XFEM method with experimental validation. Adv. Eng. Softw. 123, 1–12. https://doi.org/10.1016/j.advengsoft.2018.05.009.

Xia, H., Tan, C., Tian, R., Meng, S., Li, L., Ma, N., 2020. Influence of shielding gas on microstructure and mechanical properties of laser welded–brazed Al/Steel lapped joint. J. Manuf. Process. 54, 347–358. https://doi.org/10.1016/j.jmapro.2020.03.030.

Xian, X., Ma, Y., Shan, H., Niu, S., Li, Y., 2019. Single-sided joining of aluminum alloys using friction self-piercing riveting (F-SPR) process. J. Manuf. Process. 38, 319–327. https://doi.org/10.1016/j.jmapro.2019.01.037.

Yang, B., Shan, H., Han, X., Lin, S., Ma, Y., Lou, M., Wang, X., Li, Y., 2022. Single-sided friction riveting process of aluminum sheet to profile structure without prefabricated hole. J. Mater. Process. Technol. 307, 117663. https://doi.org/10.1016/j.jmatprotec.2022.117663.

Zhang, P., Zhao, S.D., Zhang, C.W., Zang, S.L., Chen, Z., Fei, L.Y., Wang, Y.F., Jiang, H., Zhou, H., 2022. Bonding mode and mechanical properties of keyhole-free friction stir rivet welded aluminum alloy joints. J. Mater. Res. Technol. 18, 185–199. https://doi.org/10.1016/j.jmrt.2022.02.097.

ZVEI e.V. und Bayern Innovativ GmbH, 2024. Technischer Leitfaden - Ausfallraten Für Bordnetz-Komponenten im Automobil - Erwartungswerte Und Bedingungen. ZVEI e. V. Fachverband Kabel und isolierte Drähte. https://www.zvei.org/presse-medien/publikationen/ausfallraten-fuer-bordnetz-komponenten-im-automobil. Accessed 20 June.